The $D(D_3)$-anyon chain: integrable boundary conditions and excitation spectra

Peter E. Finch and Holger Frahm

Institut für Theoretische Physik,
Leibniz Universität Hannover,
Appelstraße 2, 30167 Hannover, Germany

Abstract

Chains of interacting non-Abelian anyons with local interactions invariant under the action of the Drinfeld double of the dihedral group D_3 are constructed. Formulated as a spin chain the Hamiltonians are generated from commuting transfer matrices of an integrable vertex model for periodic and braided as well as open boundaries. A different anyonic model with the same local Hamiltonian is obtained within the fusion path formulation. This model is shown to be related to an integrable fusion interaction round the face model. Bulk and surface properties of the anyon chain are computed from the Bethe equations for the spin chain. The low energy effective theories and operator content of the models (in both the spin chain and fusion path formulation) are identified from analytical and numerical studies of the finite size spectra. For all boundary conditions considered the continuum theory is found to be a product of two conformal field theories. Depending on the coupling constants the factors can be a Z_4 parafermion or a $\mathcal{M}_{(5,6)}$ minimal model.

Contents

1 Introduction

In recent years there has been a surge of attention directed towards the understanding of many-particle systems exhibiting topological order, i.e. phases which cannot be characterised by a local order parameter. Possible realisations of such topological quantum liquids in condensed matter physics are the fractional quantum Hall (FQH) states [39, 45] and certain two-dimensional frustrated quantum magnets [5, 35, 44]. The excitations in these systems display anyonic statistics and understanding their collective behaviour is essential for the classification of topological phase transitions. Particularly interesting are non-Abelian anyons where the interchange of two particles is described by non-trivial representations of the braid group complemented by fusion rules for the decomposition of product states. The fact that these non-Abelian anyons are protected by their topological charge has led to proposals for the use of such systems in universal quantum computation [36, 46].

Some insight into the peculiar properties of many interacting anyons can be obtained in the context of simple model systems: such models can be obtained by associating anyonic degrees of freedom with each site of a lattice and defining interactions compatible with their braiding and fusion rules [17]. The phase diagram of the resulting lattice models can be studied based on the numerical computation of finite size spectra. This approach is particularly powerful for anyonic chains, i.e. one-dimensional lattices, where the numerical data can be compared against predictions from conformal field theory (CFT). Another approach, also in one dimension, makes use of the fact that the lattice model may become integrable for particular choices of coupling constants. For the solution of such models various analytical methods, e.g. in the framework of the Quantum Inverse Scattering Method (QISM), have been established which allow to study the spectrum of their low-energy excitations, their thermodynamical properties including the long-distance asymptotics of correlation functions and even form factors [37, 38].

So far much of the work on such lattice models has been focussed on systems of the non-Abelian Ising or Fibonacci anyons related to the quasiparticles in certain FQH states and their generalisations appearing in $su(2)_k$ Chern-Simons theories [4, 17, 28, 40, 53, 54]. These anyons have relatively simple fusion rules which allows for tractable computation of systems with nearest and next-nearest neighbour interactions. Integrable points within the one-dimensional versions of these models have been identified with restricted solid-on-solid (RSOS) or interaction round the face (IRF) models constructed from representations of Temperley-Lieb algebras [17, 33, 32]. An alternative method to define an anyonic theory is via the Drinfeld doubles of a finite group algebra, $D(G)$, and its representations [12]. The quasi-particles in these systems are irreducible representations (irreps) of $D(G)$ labelled by their flux, i.e. an element of $h \in G$, and their topological charge determined by the transformation properties under the residual global symmetry commuting with the flux h.

Being a quasi-triangular Hopf algebra the quantum double allows for a direct construction of integrable quantum chains with nearest neighbour interactions described by a local Hamiltonian which is invariant under the corresponding symmetry [11, 18]: within the QISM one obtains quantum spin chains on a Hilbert space being a tensor product of the finite-dimensional local spaces corresponding to a spin S, a qudit or a more general n-state quantum system. On the

other hand, it is already known that for any given model whose local Hamiltonian has the symmetry of a quasi-triangular Hopf algebra associated with an anyonic theory, it is possible to construct quantum chains using the fusion path formalism [19]. Here the basis vectors are composed of sequences of anyons and we shall refer to this as a fusion path chain. The local Hamiltonian is formally identical in the spin and the fusion path formalism. Therefore, one should expect the bulk properties of the spin and the fusion path model to be the same. The finite size spectrum of low energy excitations, however, is known to depend on boundary conditions [3, 8] and therefore should differ between the two realisations.

In this paper we study this problem for a specific one-dimensional anyon chain with nearest-neighbour interactions. The underlying symmetry of the Hamiltonian is that of the Drinfeld double of a dihedral group, specifically $D(D_3)$. In the following section we define this algebra and recall its irreps and the corresponding fusion rules. Then, using the spin basis, integrable models are constructed subject to periodic, braided and open boundary conditions, all of which being based on the usual QISM transfer matrix. In the fusion path basis we use the approach of the previous work and find a fusion IRF transfer matrix whose series expansion contains the global one-dimensional Hamiltonian. In Section 3 we compute the bulk and surface properties of the model from the Bethe ansatz formulation of the spectral properties for the spin chain. The conformal field theory and operator content for the periodic spin chain version of the $D(D_3)$ model has been identified previously [20]. In Section 4 we expand this work providing more details on the analysis as well as extending the study of the finite-size spectrum to the spin chain with braided and open boundary conditions. In addition we present numerical results for the fusion path chain in support of the expectation that the low energy excitations of the $D(D_3)$-anyon chain are described by the same CFT for all types of boundary conditions studied here.

2 The Model and its Symmetries

2.1 The $D(D_3)$ algebra

The model we consider in this article has the underlying symmetry of the Drinfeld (or quantum) double of a finite group algebra. The finite group we utilise is the dihedral group of order six, D_3, and is isomorphic to group of permutations on three elements, S_3. This group is based upon the symmetries of an equilateral triangle and has the presentation,

$$D_3 \quad = \quad \{\sigma, \tau | \sigma^3 = \tau^2 = \sigma\tau\sigma\tau = e\},$$

where e is the identity element of the group, σ is a rotation and τ is a flip. The Drinfeld double of this group is defined as the vector space,

$$D(D_3) \quad = \quad \mathbb{C}\{gh^* | g, h \in D_3\},$$

where $*$ denotes an element from the dual space of $\mathbb{C}D_3$. This space forms a quasi-triangular Hopf algebra when equipped with the multiplication and coproduct,

$$g_1 h_1^* g_2 h_2^* = \delta_{(h_1 g_2)}^{(g_2 h_2)} \, (g_1 g_2) h_2^* \quad \text{and} \quad \Delta(gh^*) = \sum_{k \in D_3} g(k^{-1}h)^* \otimes gk^*.$$

The remaining structure is uniquely determined by these relations [9, 41]. This algebra has an associated universal R-matrix i.e. an algebraic solution to the Yang–Baxter equation.

Representations

The representation theory of the Drinfeld doubles of finite group algebras are well known [14, 30]. The irreducible representations of $D(D_3)$ are classified by the conjugacy classes of D_3. The irreps associated with the conjugacy class $\{e\}$ are:

$$\begin{array}{lllllllll} \pi^{(e,\pm)}(\sigma) & = & 1 & & \pi^{(e,\pm)}(\tau) & = & \pm 1 & & \pi^{(e,\pm)}(g^*) & = & \delta_g^e \\ \pi^{(e,1)}(\sigma) & = & \begin{pmatrix} \omega & 0 \\ 0 & \omega^{-1} \end{pmatrix} & & \pi^{(e,1)}(\tau) & = & \begin{pmatrix} 0 & 1 \\ 1 & 0 \end{pmatrix} & & \pi^{(e,1)}(g^*) & = & \begin{pmatrix} \delta_g^e & 0 \\ 0 & \delta_g^e \end{pmatrix}, \end{array}$$

where $\omega = e^{\frac{2i\pi}{3}}$. The irreps associated with the conjugacy class $\{\sigma, \sigma^2\}$ are:

$$\pi^{(\sigma,k)}(\sigma) = \begin{pmatrix} \omega^k & 0 \\ 0 & \omega^{-k} \end{pmatrix} \quad \pi^{(\sigma,k)}(\tau) = \begin{pmatrix} 0 & 1 \\ 1 & 0 \end{pmatrix} \quad \pi^{(\sigma,k)}(g^*) = \begin{pmatrix} \delta_g^\sigma & 0 \\ 0 & \delta_g^{\sigma^2} \end{pmatrix},$$

where $k \in \{0, 1, 2\}$. The irreps associated with the conjugacy class $\{\tau, \sigma\tau, \sigma^2\tau\}$ are:

$$\pi^{(\tau,\pm)}(\sigma) = \begin{pmatrix} 0 & 0 & 0 \\ 0 & 0 & 0 \\ 0 & 0 & 0 \end{pmatrix} \quad \pi^{(\tau,\pm)}(\tau) = \pm \begin{pmatrix} 1 & 0 & 0 \\ 0 & 0 & 1 \\ 0 & 1 & 0 \end{pmatrix} \quad \pi^{(\tau,\pm)}(g^*) = \begin{pmatrix} \delta_g^\tau & 0 & 0 \\ 0 & \delta_g^{\sigma^2\tau} & 0 \\ 0 & 0 & \delta_g^{\sigma\tau} \end{pmatrix}.$$

The anyonic theory corresponding with $D(D_3)$ associates an irrep with an anyon [12]. For convenience it is simpler to denote each irreps by a single letter, $\mathfrak{a}, ..., \mathfrak{h}$. We equate

$$\mathfrak{a} = (e, +),\ \mathfrak{b} = (e, -),\ \mathfrak{c} = (e, 1),\ \mathfrak{d} = (\sigma, 0),\ \mathfrak{e} = (\sigma, 1),\ \mathfrak{f} = (\sigma, 2),\ \mathfrak{g} = (\tau, +),\ \mathfrak{h} = (\tau, -)$$

Properties of the anyons are inherited from their associated irreps, e.g. the dimension of an anyon equals the dimension of its corresponding irrep.

Fusion Rules

Required for an anyonic theory are the fusion rules of particles. These rules are defined by the tensor product decompositions of the associated irreps:

$\otimes$	$\mathfrak{a}$	$\mathfrak{b}$	$\mathfrak{c}$	$\mathfrak{d}$	$\mathfrak{e}$	$\mathfrak{f}$	$\mathfrak{g}$	$\mathfrak{h}$
$\mathfrak{a}$	$\mathfrak{a}$	$\mathfrak{b}$	$\mathfrak{c}$	$\mathfrak{d}$	$\mathfrak{e}$	$\mathfrak{f}$	$\mathfrak{g}$	$\mathfrak{h}$
$\mathfrak{b}$	$\mathfrak{b}$	$\mathfrak{a}$	$\mathfrak{c}$	$\mathfrak{d}$	$\mathfrak{e}$	$\mathfrak{f}$	$\mathfrak{h}$	$\mathfrak{g}$
$\mathfrak{c}$	$\mathfrak{c}$	$\mathfrak{c}$	$\mathfrak{a} \oplus \mathfrak{b} \oplus \mathfrak{c}$	$\mathfrak{e} \oplus \mathfrak{f}$	$\mathfrak{d} \oplus \mathfrak{f}$	$\mathfrak{d} \oplus \mathfrak{e}$	$\mathfrak{g} \oplus \mathfrak{h}$	$\mathfrak{g} \oplus \mathfrak{h}$
$\mathfrak{d}$	$\mathfrak{d}$	$\mathfrak{d}$	$\mathfrak{e} \oplus \mathfrak{f}$	$\mathfrak{a} \oplus \mathfrak{b} \oplus \mathfrak{d}$	$\mathfrak{c} \oplus \mathfrak{f}$	$\mathfrak{c} \oplus \mathfrak{e}$	$\mathfrak{g} \oplus \mathfrak{h}$	$\mathfrak{g} \oplus \mathfrak{h}$
$\mathfrak{e}$	$\mathfrak{e}$	$\mathfrak{e}$	$\mathfrak{d} \oplus \mathfrak{f}$	$\mathfrak{c} \oplus \mathfrak{f}$	$\mathfrak{a} \oplus \mathfrak{b} \oplus \mathfrak{e}$	$\mathfrak{c} \oplus \mathfrak{d}$	$\mathfrak{g} \oplus \mathfrak{h}$	$\mathfrak{g} \oplus \mathfrak{h}$
$\mathfrak{f}$	$\mathfrak{f}$	$\mathfrak{f}$	$\mathfrak{d} \oplus \mathfrak{e}$	$\mathfrak{c} \oplus \mathfrak{e}$	$\mathfrak{c} \oplus \mathfrak{d}$	$\mathfrak{a} \oplus \mathfrak{b} \oplus \mathfrak{f}$	$\mathfrak{g} \oplus \mathfrak{h}$	$\mathfrak{g} \oplus \mathfrak{h}$
$\mathfrak{g}$	$\mathfrak{g}$	$\mathfrak{h}$	$\mathfrak{g} \oplus \mathfrak{h}$	$\mathfrak{g} \oplus \mathfrak{h}$	$\mathfrak{g} \oplus \mathfrak{h}$	$\mathfrak{g} \oplus \mathfrak{h}$	$\mathfrak{a} \oplus \mathfrak{c} \oplus \mathfrak{d} \oplus \mathfrak{e} \oplus \mathfrak{f}$	$\mathfrak{b} \oplus \mathfrak{c} \oplus \mathfrak{d} \oplus \mathfrak{e} \oplus \mathfrak{f}$
$\mathfrak{h}$	$\mathfrak{h}$	$\mathfrak{g}$	$\mathfrak{g} \oplus \mathfrak{h}$	$\mathfrak{g} \oplus \mathfrak{h}$	$\mathfrak{g} \oplus \mathfrak{h}$	$\mathfrak{g} \oplus \mathfrak{h}$	$\mathfrak{b} \oplus \mathfrak{c} \oplus \mathfrak{d} \oplus \mathfrak{e} \oplus \mathfrak{f}$	$\mathfrak{a} \oplus \mathfrak{c} \oplus \mathfrak{d} \oplus \mathfrak{e} \oplus \mathfrak{f}$

2.2 Local Spin Hamiltonians

The $D(D_3)$ model is constructed by taking a special case of the three state Fateev–Zamolodchikov model [16]. This limit yields the R-matrix, which can also be constructed from the $\pi_{\mathfrak{g}} \otimes \pi_{\mathfrak{g}}$ representation of $D(D_3)$ [18],

$$R(z_1, z_2) = N(z_1, z_2) \sum_{a,b,i,j=0}^{2} \left[w^{(i-j)(a-b)} \overline{W}(z_1|a) \overline{W}(z_2^{-1}|b) \right] e_{i+a+b,i} \otimes e_{j+a+b,j}, \qquad (1)$$

where $e_{i,j}$ represents a 3×3 matrix (whose indices are considered modulo three) with an one in the ith row and jth column and zeros elsewhere,

$$\overline{W}(z|l) = \left[\frac{z-1}{wz-w^2}\right]^{1-\delta_l^0} \qquad \text{and} \qquad N(z_1,z_2) = -\frac{1}{3}(wz_1 - w^2)(w - w^2 z_2).$$

The R-matrix satisfies a Yang-Baxter equation in both spectral parameters,

$$R_{12}(x_1,x_2)R_{23}(x_1y_1,x_2y_2)R_{12}(y_1,y_2) \;=\; R_{23}(y_1,y_2)R_{12}(x_1y_1,x_2y_2)R_{23}(x_1,x_2), \qquad (2)$$

and has the symmetry of $D(D_3)$, implying that the operator can be expressed in terms of projection operators. The projection operators from the $\pi_{\mathfrak{g}} \otimes \pi_{\mathfrak{g}}$ to the irreps in its decomposition are,

$$p^{(a)} \;=\; \frac{\dim(a)}{6} \sum_{g,h} \mathrm{tr}[\pi_a(h^* g^{-1})](\pi_{\mathfrak{g}} \otimes \pi_{\mathfrak{g}})\Delta(gh^*),$$

where tr is the trace. In terms of these projection operators the R-matrix is written as,

$$R(z_1,z_2) \;=\; f_{\mathfrak{a}}(z_1,z_2)p^{(\mathfrak{a})} + f_{\mathfrak{c}}(z_1,z_2)p^{(\mathfrak{c})} + f_{\mathfrak{d}}(z_1,z_2)p^{(\mathfrak{d})} + f_{\mathfrak{e}}(z_1,z_2)p^{(\mathfrak{e})} + f_{\mathfrak{f}}(z_1,z_2)p^{(\mathfrak{f})}, \quad (3)$$

where

$$f_a(z_1,z_2)p^{(a)} = R(z_1,z_2)p^{(a)}, \qquad\qquad a \in \{\mathfrak{a},\mathfrak{c},\mathfrak{d},\mathfrak{e},\mathfrak{f}\}.$$

This R-matrix will allow the construction of integrable models subject to various boundary conditions. Due to the two spectral parameters present two local Hamiltonians are obtained in the usual manner,

$$h^{(k)} \;=\; i\frac{d}{dz_k}R(z_1,z_2) - \beta_k I \otimes I,$$

where $k \in \{1,2\}$ and $\beta_k \in \mathbb{C}$ is chosen such that the trace of the local Hamiltonians is zero. We find that,

$$\begin{aligned} h^{(1)} &= \frac{2\sqrt{3}}{3}p^{(\mathfrak{a})} - \frac{\sqrt{3}}{3}p^{(\mathfrak{c})} - \frac{\sqrt{3}}{3}p^{(\mathfrak{d})} - \frac{\sqrt{3}}{3}p^{(\mathfrak{e})} + \frac{2\sqrt{3}}{3}p^{(\mathfrak{f})}, \qquad (4)\\ h^{(2)} &= \frac{2\sqrt{3}}{3}p^{(\mathfrak{a})} - \frac{\sqrt{3}}{3}p^{(\mathfrak{c})} - \frac{\sqrt{3}}{3}p^{(\mathfrak{d})} + \frac{2\sqrt{3}}{3}p^{(\mathfrak{e})} - \frac{\sqrt{3}}{3}p^{(\mathfrak{f})}. \end{aligned}$$

It follows that the local Hamiltonians commute with each other and with the action of the algebra:

$$\left[h^{(1)}, h^{(2)}\right] = 0 \quad \text{and} \quad \left[(\pi_{\mathfrak{g}} \otimes \pi_{\mathfrak{g}})\Delta(a), h^{(k)}\right] = 0,$$

for all $a \in D(D_3)$. Therefore they have the underlying symmetry of $D(D_3)$ as the R-matrix did. In this basis we have that $h^{(1)}$ and $h^{(2)}$ are related,

$$h^{(1)} = \Pi h^{(2)} \Pi = \left[h^{(2)}\right]^*$$

where Π is usual two-site permutation operator and $*$ is, and herein reserved for, complex conjugation. Both local Hamiltonians are self-adjoint.

2.3 Global Hamiltonian

We consider a variety of different models which differ only by boundary conditions. For every case the global Hamiltonian is comprised of two components in the following way,

$$\mathcal{H}_\theta \quad = \quad \cos(\theta)\,\mathcal{H}^{(1)} + \sin(\theta)\,\mathcal{H}^{(2)}. \tag{5}$$

The presence of the coupling parameter is due to the two distinct local Hamiltonians. For all boundary conditions considered the integrability of the global Hamiltonians is ensured by the existence of a commuting transfer matrix. Furthermore the two components of each global Hamiltonian will commute,

$$\left[\mathcal{H}^{(1)}, \mathcal{H}^{(2)}\right] \quad = \quad 0. \tag{6}$$

This commutativity allows us to investigate the individual spectra of $\mathcal{H}^{(1)}$ and $\mathcal{H}^{(2)}$. Typically the spectra of $\mathcal{H}^{(1)}$ and $\mathcal{H}^{(2)}$ will be identical or of a related form.

2.3.1 Periodic Spin Chain

We begin by considering the $D(D_3)$ model as a spin chain with periodic boundary conditions: its global Hamiltonians are defined by

$$\mathcal{H}^{(k)} \quad = \quad h^{(k)}_{\mathcal{L}0} + \sum_{j=1}^{\mathcal{L}-1} h^{(k)}_{j(j+1)},$$

for $k \in \{1, 2\}$. Note that the periodic closure by the term $h^{(k)}_{\mathcal{L}0}$ in the global Hamiltonian breaks the $D(D_3)$ invariance of the model. Both of these Hamiltonians appear in the series expansion of the commuting transfer matrix [38],

$$t(z_1, z_2) \quad = \quad \mathrm{tr}_0\left[\Pi_{0\mathcal{L}} R_{0\mathcal{L}}(z_1, z_2^*) \cdots \Pi_{01} R_{01}(z_1, z_2^*)\right].$$

By construction this transfer matrix is a polynomial of degree $\mathcal{L}$ in the variables z_1 and z_2^*. It has been observed that this transfer matrix factorises and that its eigenvalues are always of the form

$$\Lambda(z_1, z_2) \quad = \quad c \prod_{\ell=1}^{\mathcal{L}} (z_1 - z_{1,\ell}) \prod_{\ell=1}^{\mathcal{L}} (z_2 - z_{2,\ell})^*. \tag{7}$$

Therefore the eigenvalues can be conveniently described in terms of their zeroes $z_{k,\ell} \equiv i\omega \mathrm{e}^{x_{k,\ell}}$, for $k = 1, 2$ and $\ell = 1, \ldots, \mathcal{L}$. The two sets of parameters $\{x_{k,\ell}\}_{\ell=1}^{\mathcal{L}}$ independently satisfy the Bethe equations [21]

$$(-1)^{\mathcal{L}+1} \left(\frac{1 + (i/\omega)\mathrm{e}^{x_{k,j}}}{1 - i\omega\,\mathrm{e}^{x_{k,j}}}\right)^{\mathcal{L}} = \prod_{l=1}^{\mathcal{L}} \frac{\mathrm{e}^{x_{k,l}} - (1/\omega)\mathrm{e}^{x_{k,j}}}{\mathrm{e}^{x_{k,l}} - \omega\,\mathrm{e}^{x_{k,j}}}, \quad j = 1, \ldots, \mathcal{L}. \tag{8}$$

The energy eigenvalue of $\mathcal{H}^{(k)}$ corresponding to the set of Bethe roots $\{x_{k,\ell}\}$ is given by

$$E^{(k)} \equiv E(\{x_{k,\ell}\}) = i\left[\sum_{\ell=1}^{\mathcal{L}} \frac{1}{1 - i\omega e^{x_{k,\ell}}} - \frac{1}{6}\left(3 + i\sqrt{3}\right)\mathcal{L}\right], \tag{9}$$

where we have used property sets of Bethe roots are invariant under complex conjugations, $\{x_{k,\ell}\}_{\ell=1}^{\mathcal{L}} \equiv \{x_{k,\ell}^*\}_{\ell=1}^{\mathcal{L}} \pmod{2i\pi}$. It is important note that while there are exactly $\mathcal{L}$ Bethe roots in each set $\{x_{k,\ell}\}_{\ell=1}^{\mathcal{L}}$, they are allowed to be at $\pm\infty$, but at most one at each. These roots need to be recorded and dealt with appropriately to ensure the energy is real.

Let us remark that the Bethe equations (8) and the corresponding energies (9) of the $D(D_3)$ spin chain of even length $\mathcal{L}$ coincide with those of the three-state Potts spin chain with $\mathcal{L}/2$ sites [2]. We shall use this equivalence below to identify some of the thermodynamical properties of the $D(D_3)$ chain.

The energy eigenvalues of the *complete* Hamiltonian are characterised by two solutions to the Bethe equations (8). As a consequence of Equations (5,6) and along with (9) they are given by

$$E = \cos(\theta)\, E^{(1)} + \sin(\theta)\, E^{(2)} = \cos(\theta)\, E(\{x_{1,\ell}\}) + \sin(\theta)\, E(\{x_{2,\ell}\}), \tag{10}$$

provided these energies pair. Specifically, levels are said to pair if the two corresponding sets of Bethe roots form an eigenvalue of the transfer matrix, see Equation (7). As the two sets of Bethe roots need not correspond to a unique eigenvalue of the transfer matrix, e.g. there may be two eigenvalues that differ by a constant factor or an eigenvalue might be degenerate, we refer to the total number of eigenvalues, including degeneracies, as the *pairing multiplicity*.

The total momentum of the corresponding state can also be given in terms of the two sets of Bethe roots: at $z_1 = 1 = z_2$ the transfer matrix becomes a shift operator by one site, therefore the momentum operator is $P = -i \ln t(1,1)$. Unlike for the energy (9) the partial momentum contribution from one of the participating Bethe configurations cannot be defined uniquely [21]. By construction the eigenvalues of P are real ($2\pi/\mathcal{L}$ times an integer for periodic boundary conditions considered here). Therefore we may define the partial and complete momenta to be

$$\begin{aligned} P^{(k)} &\equiv P(\{x_{k,\ell}\}) = \mathrm{Re}\left[\frac{1}{i}\sum_{\ell} \ln(1 - iwe^{x_{k,\ell}})\right], \\ P &= P^{(1)} - P^{(2)} + \text{const.}. \end{aligned} \tag{11}$$

Again, roots $x_{k,\ell} = \pm\infty$ have to be taken into account to ensure finite (partial) momentum. The total momentum is given by the difference of partial momenta reflecting the fact $\mathcal{H}^{(2)}$ is the spatial inversion of $\mathcal{H}^{(1)}$. The remaining constant represents a macroscopic effect, details of which have been discussed in earlier works [21].

2.3.2 Braided Chain

One closed chain proposed as an alternative to the periodic chain is the braided chain [22, 31, 34]. In this model, translational invariance is replaced by invariance under a global braiding operator. As a consequence the underlying symmetry of the model will not be broken, i.e. it has the full global $D(D_3)$ symmetry. The global Hamiltonians are defined by,

$$\mathcal{H}^{(k)} = B h^{(k)}_{(\mathcal{L}-1)\mathcal{L}} B^{-1} + \sum_{j=1}^{\mathcal{L}-1} h^{(k)}_{j(j+1)}, \qquad k \in \{1,2\},$$

where

$$B = b_{12} b_{23} ... b_{(\mathcal{L}-1)\mathcal{L}}, \qquad \text{and} \qquad b = \lim_{z\to\infty}\left[\frac{1}{z^2} R(z,z)\right].$$

There are different possible definitions for the braiding operator b_i relating to other limits of $R(z_1, z_2)$ which we do not consider within this article. The integrability of the model is ensured by the existence of a transfer matrix $t(z_1, z_2)$, which can be found in [18]. Eigenstates of this model are again characterised by the Bethe Equations (8). Again there must be $\mathcal{L}$ Bethe roots, this time with one Bethe root allowed at $+\infty$ but none allowed at $-\infty$. In this case we find $t(1,1) = B$. Calculating the order of B for small system sizes we find that

$$B^n = I^{\otimes \mathcal{L}}, \quad \text{when} \begin{cases} n = 3\mathcal{L}, & \mathcal{L} \text{ even}, \\ n = 2\mathcal{L}, & \mathcal{L} \text{ odd}. \end{cases}$$

This allows us to define a generator of translation, $P = -i \ln B$. The eigenvalues of P are restricted to integer multiples of either $\frac{\pi}{\mathcal{L}}$ or $\frac{2\pi}{3\mathcal{L}}$ depending on the parity of $\mathcal{L}$.

2.3.3 Open Boundary Conditions

We also consider spin chains with open boundary conditions. The reflection matrices, i.e. K-matrices, required for the construction of an open chain whose boundary fields preserve integrability [51] are the same as have been determined for the $D(D_3)$ one-parameter R-matrix [10]. The global Hamiltonians are,

$$\mathcal{H}^{(k)} = \chi_k^- B_1^{(k)-} + \chi_k^+ B_{\mathcal{L}}^{(k)+} + \sum_{j=1}^{\mathcal{L}-1} h_{j(j+1)}^{(k)} .$$

The boundary operators $B^{(k)-}$ ($B^{(k)+}$) act on the first (last) site of the chain, respectively. There are three possible (independent) options for each of the different boundary operators,

$$B^{(1)-}, (B^{(1)+})^*, (B^{(2)-})^*, B^{(2)+} \in \left\{ \left(\begin{array}{ccc} 0 & w^2 b & w^2 b^2 \\ w b^2 & 0 & b \\ w b & b^2 & 0 \end{array} \right) \middle| \, b = 1, w, w^2 \right\} .$$

The real boundary amplitudes where $\chi_k^{\pm}$, $k \in \{1, 2\}$, have to satisfy $\chi_1^+ \chi_2^+ = \chi_1^- \chi_2^- = 0$. Like the periodic and braided models integrability is derived from the existence of a transfer matrix (see [18, 21] for the open $D(D_3)$ transfer matrix) and the eigenstates of the Hamiltonian are classified by sets of Bethe roots. The Bethe equations for the Hamiltonian $\mathcal{H}^{(k)}$ are independent of the choice of the boundary operators, $B^{(k)\pm}$,

$$\begin{aligned} \prod_{l=1}^{d_k} \left(\frac{e^{x_{k,l}} - \omega^2 e^{x_{k,j}}}{e^{x_{k,l}} - \omega e^{x_{k,j}}} \right) &= (-1)^{\mathcal{L}+1} \left(\frac{1 + \omega e^{2x_{k,j}}}{1 + \omega^2 e^{2x_{k,j}}} \right) \left(\frac{1 - \omega^2 e^{2x_{k,j}}}{1 - \omega e^{2x_{k,j}}} \right) \left(\frac{1 + i\omega^2 e^{x_{k,j}}}{1 - i\omega e^{x_{k,j}}} \right)^{2\mathcal{L}} \\ &\quad \times \Phi(x_{k,j}, \chi_k^-) \Phi(x_{k,j}, \chi_k^+) \end{aligned}$$

with Bethe roots always appearing in pairs of $\pm x$ and where

$$\Phi(x_{k,j}, \chi_k^{\pm}) = \begin{cases} 1, & \chi_k^{\pm} = 0, \\ \left(\frac{\chi_k^{\pm}\sqrt{3}(1 - \omega e^{2x_{k,j}}) + i\omega^2 \left(1 + \chi_k^{\pm}\sqrt{3}\right) e^{x_{k,j}}}{\chi_k^{\pm}\sqrt{3}(1 - \omega^2 e^{2x_{k,j}}) - i\omega \left(1 + \chi_k^{\pm}\sqrt{3}\right) e^{x_{k,j}}} \right), & \chi_k^{\pm} \neq 0. \end{cases}$$

As the Bethe equations depend on the parameters $\chi_k^{\pm}$ so do the number of Bethe roots. If $\chi_k^{\pm} = 0$ then we obtain the open chains with free-ends, in which case we have $d_k = 2\mathcal{L}$ Bethe roots with

at most one pair of roots at $\pm\infty$. We refer to this Hamiltonian as the bulk Hamiltonian and describe the Bethe roots of the system as belonging to the bulk. If only one of either χ_k^+ or χ_k^- is non-zero then there are $d_k = 2\mathcal{L}+2$ Bethe roots, while if both χ_k^+ and χ_k^- are non-zero then there are $d_k = 2\mathcal{L}+4$ Bethe roots. The extra pairs of Bethe roots appearing, as compared to the free-ends case, are referred to as boundary Bethe roots[1]. The boundary Bethe roots are always finite but approach $\pm\infty$ in pairs as $\chi_k^\pm$ approaches zero. The energy of the $\mathcal{H}^{(k)}$ Hamiltonian corresponding to a set of Bethe roots is given by

$$E^{(k)}(\{x_{k,\ell}\}) \;=\; \frac{i}{2}\left\{\sum_{l=1}^{d_k}\left[\frac{1}{1-iwe^{x_{k,l}}}\right] - (1-i\frac{\sqrt{3}}{3})\mathcal{L} - \phi(\chi_k^+) - \phi(\chi_k^-)\right\},$$

where

$$\phi(\chi_k^\pm) \;=\; \begin{cases} 0, & \chi_k^\pm = 0, \\ 1+i\chi_k^\pm & \chi_k^\pm \neq 0, \end{cases}$$

Only when the boundary interactions are not present, i.e. with free-ends, will the model have $D(D_3)$ invariance.

2.4 Fusion Path Analogues

As the local Hamiltonians have the symmetry of $D(D_3)$ it is possible to create fusion path analogues [19]. Depending on the boundary conditions imposed the global Hamiltonians may or may not be equivalent to their spin formalism counterparts. The construction of the analogous fusion path chains uses the same method of Pasquier's representation theory reliant face-vertex correspondence [49]. This allows the fusion path analogues to be considered as the Hamiltonian limits of RSOS models and proves their integrability. The connection between fusion IRF models and many other physical systems has already been established [25].

We first define the fusion path basis. Basis vectors of the fusion path space are of the form,

$$|a_0 a_1 ... a_{\mathcal{L}}\rangle\,,$$

where $a_i \in \{\mathfrak{a},\mathfrak{b},\mathfrak{c},\mathfrak{d},\mathfrak{e},\mathfrak{f},\mathfrak{g},\mathfrak{h}\}$ and neighbouring labels satisfy the condition,

$$\begin{aligned} a_i a_{i+1} \;&\in\; \{ab \,|\, V_b \subset V_a \otimes V_{\mathfrak{g}}\} \\ &=\; \{\mathfrak{ag},\mathfrak{bh},\mathfrak{cg},\mathfrak{ch},\mathfrak{dg},\mathfrak{dh},\mathfrak{eg},\mathfrak{eh},\mathfrak{fg},\mathfrak{fh}, \\ &\quad\; \mathfrak{ga},\mathfrak{gc},\mathfrak{gd},\mathfrak{ge},\mathfrak{gf},\mathfrak{hb},\mathfrak{hc},\mathfrak{hd},\mathfrak{he},\mathfrak{hf}\}. \end{aligned} \tag{12}$$

Thus a_{i+1} must appear in the fusion of a_i and $\mathfrak{g}$. Diagrammatically a basis vector corresponds to the figure below, where the joining of two lines indicates fusion which occurs from top-left to bottom-right,

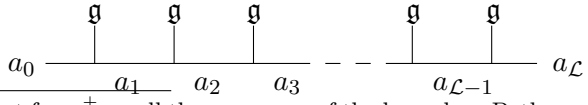

[1]It is important to note that for $\chi_k^\pm$ small the presences of the boundary Bethe roots will not have a significant effect on the configuration of the bulk Bethe roots.

To construct operators on this space we utilise F-moves (generalised 6-j symbols), which allow the temporary re-ording of fusion,

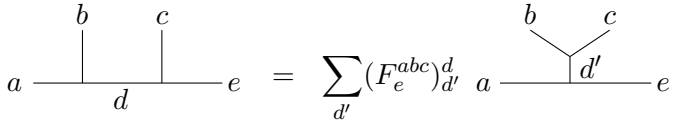

These F-moves are required to construct the projection operators acting on a bond[2],

$$\tilde{p}^{(b)}_{i-1,i,i+1} = \sum_{a_{i-1},a_i,a_i',a_{i+1}} \left[\left(F^{a_{i-1}\mathfrak{gg}}_{a_{i+1}}\right)^{a_i'}_{b}\right]^* \left(F^{a_{i-1}\mathfrak{gg}}_{a_{i+1}}\right)^{a_i}_{b} \left|..a_{i-1}a_i'a_{i+1}..\right\rangle \left\langle..a_{i-1}a_ia_{i+1}..\right|.$$

where the coefficients F are the unitary F-moves associated with $D(D_3)$. These can be calculated explicitly from the representation theory of $D(D_3)$, however, as they are not essential we omit them. Below we shall consider local interactions defined analogously to Equation (4):

$$\begin{aligned}
\tilde{h}^{(1)} &= \frac{2\sqrt{3}}{3}\tilde{p}^{(\mathfrak{a})} - \frac{\sqrt{3}}{3}\tilde{p}^{(\mathfrak{c})} - \frac{\sqrt{3}}{3}\tilde{p}^{(\mathfrak{d})} - \frac{\sqrt{3}}{3}\tilde{p}^{(\mathfrak{e})} + \frac{2\sqrt{3}}{3}\tilde{p}^{(\mathfrak{f})} \\
\tilde{h}^{(2)} &= \frac{2\sqrt{3}}{3}\tilde{p}^{(\mathfrak{a})} - \frac{\sqrt{3}}{3}\tilde{p}^{(\mathfrak{c})} - \frac{\sqrt{3}}{3}\tilde{p}^{(\mathfrak{d})} + \frac{2\sqrt{3}}{3}\tilde{p}^{(\mathfrak{e})} - \frac{\sqrt{3}}{3}\tilde{p}^{(\mathfrak{f})}
\end{aligned}$$

These Hamiltonians act on three consecutive labels but only can change the middle label.

As a consequence of the equivalence of the local interactions between the spin and fusion path formalisms the global models in the two formalisms may differ only by boundary conditions. The open model with free ends and braided model both have $D(D_3)$ invariance which means that the fusion path and spin versions of these chains are equivalent. For periodic boundary conditions neither the spin nor fusion path formalism has the complete $D(D_3)$ invariance and thus the two models, while sharing bulk properties, are distinct [19]. For a periodic model in the fusion path basis we need to consider the space spanned by the basis vectors satisfying $a_0 = a_{\mathcal{L}}$. As a consequence of the fusion rules this periodic closure is possible for $\mathcal{L}$ even only and leads to the decomposition of the Hilbert space,

$$\text{Hilbert Space} = \mathbb{C}\left\{\left|a_1...a_{\mathcal{L}}\right\rangle \left|a_1 = \mathfrak{g} \text{ or } a_1 = \mathfrak{h}\right\}\right. \oplus \mathbb{C}\left\{\left|a_1...a_{\mathcal{L}}\right\rangle \left|a_2 = \mathfrak{g} \text{ or } a_2 = \mathfrak{h}\right\}\right., \quad (13)$$

where each of these subspaces has dimension $3^{\mathcal{L}} + 1$. The global Hamiltonians are,

$$\tilde{\mathcal{H}}^{(k)} = \tilde{h}^{(k)}_{(\mathcal{L}-1)\mathcal{L}1} + \tilde{h}^{(k)}_{\mathcal{L}12} + \sum_{j=2}^{\mathcal{L}-1} \tilde{h}^{(k)}_{(j-1)j(j+1)}, \qquad k \in \{1,2\}.$$

The integrability of this model arises from the existence of an analogous R-matrix connected to an RSOS model whose heights correspond to the labels of the irreps of $D(D_3)$. As the R-matrix of Equation (3) is expressible in terms of the $D(D_3)$ projection operators it follows that there exists an equivalent operator in the fusion path basis [49],

$$\begin{aligned}
\tilde{R}(z_1,z_2) &= f_{\mathfrak{a}}(z_1,z_2)\tilde{p}^{(\mathfrak{a})} + f_{\mathfrak{c}}(z_1,z_2)\tilde{p}^{(\mathfrak{c})} + f_{\mathfrak{d}}(z_1,z_2)\tilde{p}^{(\mathfrak{d})} + f_{\mathfrak{e}}(z_1,z_2)\tilde{p}^{(\mathfrak{e})} + f_{\mathfrak{f}}(z_1,z_2)\tilde{p}^{(\mathfrak{f})} \quad (14) \\
&= \sum_{a_1,a_2,a_2',a_3} B\left(\begin{array}{cc} a_1 & a_2' \\ a_2 & a_3 \end{array}\middle| z_1,z_2\right) \left|a_1a_2'a_3\right\rangle \left\langle a_1a_2a_3\right|,
\end{aligned}$$

[2]It is important for the reader to note that in this fusion path formalism that the labels in the basis vectors do not correspond to individual sites but rather bonds. The individual sites are still the $\mathfrak{g}$-anyons but now can not be solely acted on as this would break local $D(D_3)$ invariance.

which satisfies a face Yang-Baxter equation,

$$\tilde{R}_{123}(x_1,x_2)\tilde{R}_{234}(x_1y_1,x_2y_2)\tilde{R}_{123}(y_1,y_2) \;=\; \tilde{R}_{234}(y_1,y_2)\tilde{R}_{123}(x_1y_1,x_2y_2)\tilde{R}_{234}(x_1,x_2),$$

as $R(z_1,z_2)$ satisfies Equation (2). The weights appearing in $\tilde{R}(z_1,z_2)$ are used to construct the commuting transfer matrix [29],

$$\left\langle a'_1 ... a'_{\mathcal{L}} \right| t(z_1,z_2) \left| a_1 ... a_{\mathcal{L}} \right\rangle \;=\; \prod_{j=1}^{\mathcal{L}} B\left(\begin{array}{cc} a'_j & a'_{j+1} \\ a_j & a_{j+1} \end{array} \middle| z_1,z_2 \right).$$

Once again the global Hamiltonians is generated by this transfer matrix, with $\tilde{\mathcal{H}}^{(1)}$ and $\tilde{\mathcal{H}}^{(2)}$ appearing in its series expansion, implying integrability. The existence of the transfer matrix also guarantees commutativity of the two components

$$\left[\tilde{\mathcal{H}}^{(1)}, \tilde{\mathcal{H}}^{(2)}\right] = 0.$$

In previous anyonic fusion path models [17, 33] integrability was also shown by constructing transfer matrices associated with RSOS models, however in these instances the fusion path R-matrices corresponded to representations of the Temperley-Lieb algebra.

Every RSOS model can be naturally associated with a graph [48]. For the $D(D_3)$ model considered here we obtain the graph given in Figure 1. This graph is equivalent to McKay's representation graph for the representation $\pi_{\mathfrak{g}}$ of $D(D_3)$ [43]. The graph indicates that the $D(D_3)$ fusion path model does not correspond to any of the known (dilute) RSOS models associated with Dynkin diagrams [48, 47, 50, 56]. We notes that the graph also doesn't appear amongst the more general graphs associated with other RSOS models [13].

Figure 1: A graphical representation of allowed neighbouring labels in the fusion path chain. The vertices/nodes of the graphs are the labels of anyons which are connected via an edge if and only if the two anyon labels can appear next to each as given by Equation (12).

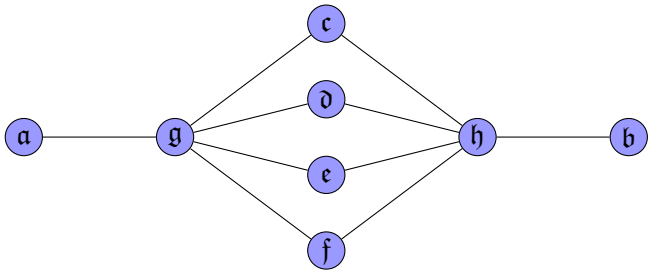

3 The Bethe Equations and Exact Results for Spin Chains

As a consequence of Eq. (10) the ground state energy of the model is always obtained by the following combinations (NB: provided that these states are allowed to pair)

$$E_0 = \begin{cases} \cos(\theta)E_l^{(1)} + \sin(\theta)E_l^{(2)}, & 0 \leq \theta < \frac{\pi}{2}, \\ \cos(\theta)E_h^{(1)} + \sin(\theta)E_h^{(2)}, & \frac{\pi}{2} \leq \theta < \pi, \\ \cos(\theta)E_h^{(1)} + \sin(\theta)E_h^{(2)}, & \pi \leq \theta < \frac{3\pi}{2}, \\ \cos(\theta)E_l^{(1)} + \sin(\theta)E_h^{(2)}, & \frac{3\pi}{2} \leq \theta < 2\pi, \end{cases} \tag{15}$$

where $E_l^{(k)}$ is the lowest energy of the $\mathcal{H}^{(k)}$ and $E_h^{(i)}$ is the highest. An immediate implication of this form of the ground state energy is that there are level-crossings for θ being integer multiples of $\frac{\pi}{2}$ leading to first order quantum phase transitions. Here we will use a different consequence of (15): the complete spectrum of the model can be obtained from an analysis at these particular points in combination with the implementation of the pairing rules [21]. An additional simplification arises from the fact that the spectra of $\mathcal{H}^{(1)}$ and $\mathcal{H}^{(2)}$ are identical for most boundary conditions considered in this paper: this allows us to restrict the analysis of the low-energy spectrum to those of the Hamiltonians $\mathcal{H}_{\theta=0} = \mathcal{H}^{(1)}$ and $\mathcal{H}_{\theta=\pi} = -\mathcal{H}^{(1)}$ whose ground state energies are $E_l^{(1)} = E_l^{(2)}$ and $-E_h^{(1)} = -E_h^{(2)}$, respectively. Only in the case of open boundary conditions with $D(D_3)$-symmetry breaking boundary fields are the spectra of $\pm\mathcal{H}^{(1)}$ and $\pm\mathcal{H}^{(2)}$ are independent.

3.1 Energy Density in the Thermodynamical Limit

In the thermodynamic limit $\mathcal{L} \to \infty$ bulk properties of the system are independent of the boundary conditions imposed. Therefore we can compute the energy density from the Bethe equations (8) for the periodic spin chain. To this end the solutions to the Bethe equations need to be classified and the root configurations corresponding to the ground state and low energy excitations have to the identified. As mentioned above, the Bethe equations for the periodic $D(D_3)$ spin chain arise also in the context of the 3-state Potts model. For the latter the classification of solutions has been obtained by Albertini *et al.* [2, 1], see also Ref. [21]. In particular, numerical diagonalisation of the transfer matrix shows that the lowest energy states of $\mathcal{H}_{\theta=\pi}$ consist of three different Bethe root ($z_l \equiv z_{1,l}$) types:

1. Positive Bethe roots (+-string), $z_l = i\omega e^{x_l^+}$, where $x_l^+ \in \mathbb{R}$,
2. Negative Bethe roots (−-string), $z_l = i\omega e^{x_l^- + i\pi}$, where $x_l^- \in \mathbb{R}$,
3. 2-strings, where the Bethe roots come in pairs, $z_l = i\omega e^{x_l^s + \frac{2i\pi}{3}}, z_{l+1} = i\omega e^{x_l^s - \frac{2i\pi}{3}}$ with $x_l^s \in \mathbb{R}$,

as well as a limited number of Bethe roots at $\pm\infty$. Letting N_+, N_- and N_2 be the number of +-strings, −-strings and 2-strings respectively and setting $n_{\pm\infty} \in \{0, 1\}$ to be the number of Bethe roots at $\pm\infty$ then we have the constraint

$$N_+ + N_- + 2N_s = \mathcal{L} - n_{+\infty} - n_{-\infty}.$$

In the 3-states Potts model these root types were also identified, along with a few other which we don't consider, with the additional constraint $n_{+\infty} = n_{-\infty}$ [2].

Allowing combinations of these roots we then find that the for the periodic Hamiltonian we can take the logarithm of the Bethe equations and define the following set of counting functions:

$$\begin{aligned}
Z_+(x) &= -\phi(x;\frac{7}{12}) + \frac{1}{\mathcal{L}}\sum_{l=1}^{N_+}\phi(x-x_l^+;\frac{1}{3}) + \frac{1}{\mathcal{L}}\sum_{l=1}^{N_-}\phi(x-x_l^-;\frac{5}{6}) + \frac{1}{\mathcal{L}}\sum_{l=1}^{N_s}\phi(x-x_l^s;\frac{2}{3}) \\
Z_-(x) &= -\phi(x;\frac{1}{12}) + \frac{1}{\mathcal{L}}\sum_{l=1}^{N_+}\phi(x-x_l^+;\frac{5}{6}) + \frac{1}{\mathcal{L}}\sum_{l=1}^{N_-}\phi(x-x_l^-;\frac{1}{3}) + \frac{1}{\mathcal{L}}\sum_{l=1}^{N_s}\phi(x-x_l^s;\frac{1}{6}) \\
Z_s(x) &= \Big[\phi(x;\frac{11}{12}) + \phi(x;\frac{1}{4})\Big] - \frac{1}{\mathcal{L}}\sum_{k=1}^{N_+}\phi(x-x_l^+;\frac{2}{3}) - \frac{1}{\mathcal{L}}\sum_{l=1}^{N_-}\phi(x-x_l^-;\frac{1}{6}) - \frac{1}{\mathcal{L}}\sum_{l=1}^{N_s}\phi(x-x_l^s;\frac{1}{3})
\end{aligned}$$

where

$$\phi(x;t) = -\frac{1}{\pi}\tan^{-1}\left(\frac{\tanh(\frac{x}{2})}{\tan(t\pi)}\right).$$

We find that the ground state for $\mathcal{H}_{\theta=\pi}$ consists entirely of 2-strings and is only realised when $\mathcal{L}$ is even.

Similarly we find that the lowest energy states of $\mathcal{H}_{\theta=0}$ consist of the three same Bethe root types and hence we have the same counting functions. However, we find that the ground state this time is only realised when $\mathcal{L}$ is a multiple of four and consists of $3\mathcal{L}/4$ negative Bethe roots and $\mathcal{L}/4$ positive Bethe roots.

Based on these observations the root density formalism [57] can be applied to compute the corresponding energy densities: The density of 2-strings in the thermodynamic ground state of $\mathcal{H}_{\theta=\pi}$ and their dressed energies $\mathcal{H}_{\theta=\pi}$ are determined by linear integral equations

$$\begin{aligned}\rho(x) &= \frac{1}{\pi}\left(\frac{1}{4\cosh(x)-2\sqrt{3}} - \frac{1}{2\cosh(x)}\right) + \frac{\sqrt{3}}{2\pi}\int_{-\infty}^{\infty}\mathrm{d}y\,\frac{1}{2\cosh(x-y)+1}\rho(y)\,,\\ \epsilon(x) &= \frac{1}{4\cosh(x)-2\sqrt{3}} - \frac{1}{2\cosh(x)} + \frac{\sqrt{3}}{2\pi}\int_{-\infty}^{\infty}\mathrm{d}y\,\frac{1}{2\cosh(x-y)+1}\epsilon(y)\,.\end{aligned} \tag{16}$$

These equations (and the corresponding ones for $H_{\theta=0}$) can be solved by Fourier transformation giving the ground state energy densities [2, 21]

$$\frac{1}{\mathcal{L}}E_{\theta=\pi} = -\left[\frac{1}{\pi}+\frac{2\sqrt{3}}{9}\right] \qquad \text{and} \qquad \frac{1}{\mathcal{L}}E_{\theta=0} = -\left[\frac{1}{2\pi}-\frac{2\sqrt{3}}{9}+\frac{3}{4}\right]. \tag{17}$$

3.2 Fermi-velocity

The low-energy excitations over these ground states have a linear dispersion and their Fermi velocities have been computed from the root density formalism in the context of the three-state Potts model [2]. The identification of the energy eigenvalues of this model with the partial spectrum of the $D(D_3)$ Hamiltonian (9) based on the equivalence of the corresponding Bethe equations however can not be extended to the spectrum of the (partial) momentum operator. Instead we use the observation that the root configurations solving the Bethe equations are invariant under complex conjugation $\{x_\ell\} \leftrightarrow \{x_\ell^*\}$ (mod $2i\pi$) to rewrite (11) as

$$P(\{x_\ell\}) = \frac{1}{2i}\sum_\ell \ln\left(\frac{1-i\omega\mathrm{e}^{x_\ell}}{1-(1/i\omega)\mathrm{e}^{x_\ell}}\right) \tag{18}$$

which is *half* of the momentum in the three state Potts chain. This implies that the contribution of a 2-string to the partial momentum is

$$P(x) = \pi\int^x \mathrm{d}y\,\rho(y) \tag{19}$$

and therefore the Fermi velocity of low lying excitations of $H_{\theta=\pi}$ is found to be

$$v_F = \frac{1}{\pi}\frac{\epsilon'(x)}{\rho(x)}\bigg|_{x=-\infty} = 3 \tag{20}$$

in agreement with the finite size analysis of the spectrum performed in [20].

Similarly we can compute the Fermi velocity of gapless excitations for the Hamiltonian H_0. Again the result is twice than what has been found for the three-state Potts chain [2], i.e. $v_F = \frac{3}{2}$.

3.3 Boundary Fields

We can also determine the exact expressions for the surface energy, i.e. the $\mathcal{L}^0$ contributions to the energy, for the open model with interacting boundary fields. Firstly we find the ground energy for the Hamiltonians $\mathcal{H}_{\theta=\pi}$ and $\mathcal{H}_{\theta=0}$, and then extend this result to generic θ. We can use the Bethe equations given in the previous section and apply the same method that was used to calculate bulk energy density, however, due to the free parameters we need to utilise certain assumptions concerning the behaviour of the boundary Bethe roots. Due to the symmetry of the Bethe equations it is enough to look at the correction to the surface energy with only one boundary field present compared to the free-ends case.

As stated earlier for $\mathcal{H}_{\theta=\pi}$ with $\chi_1^- = 0$ and $\chi_1^+ \neq 0$ there will be two additional Bethe roots present. If χ_1^+ is not too large then we find that ground state consists of $\mathcal{L}$ 2-strings (for even $\mathcal{L}$) bulk Bethe roots and two boundary Bethe roots as either $\pm$-strings depending on the sign of χ_1^+. The smaller χ_1^+ is, the larger the magnitude[3] of the boundary roots are. Using these observations we can obtain analytical expressions for the surface energy for $-\frac{1}{3\sqrt{3}} < \chi_k^{\pm} < \frac{1}{\sqrt{3}}$. We find that the correction to surface energy for the Hamiltonian $\mathcal{H}_{\theta=\pi}$ with one interacting boundary field, compared to the free ends case, is

$$g_{\theta=\pi}(\chi) = -\frac{2\chi^2\sqrt{3}}{1+2\chi\sqrt{3}} - \frac{18\chi^3\sqrt{3}}{\pi(1+2\chi\sqrt{3})\sqrt{1+2\chi\sqrt{3}-9\chi^2}} \begin{cases} \operatorname{arccosh}(-\frac{1}{2}-\frac{1}{2\chi\sqrt{3}}), & \chi<0, \\ 0, & \chi=0, \\ \operatorname{arccosh}(\frac{1}{2}+\frac{1}{2\chi\sqrt{3}}), & \chi>0. \end{cases}$$

Similarly, we find the surface energy correction for $\mathcal{H}_{\theta=0}$,

$$g_{\theta=0}(\chi) = \frac{2\chi^2\sqrt{3}}{1+2\chi\sqrt{3}} - \begin{cases} \frac{-9\chi\sqrt{-\chi}}{2(1+2\chi\sqrt{3})\sqrt{\sqrt{3}-3\chi}} + \frac{9\chi^3\sqrt{3}\operatorname{arccosh}(-\frac{1}{2}-\frac{1}{2\chi\sqrt{3}})}{\pi(1+2\chi\sqrt{3})\sqrt{1+2\chi\sqrt{3}-9\chi^2}}, & \chi<0, \\ 0, & \chi=0, \\ \frac{9\chi\sqrt{\chi}}{2\sqrt{\sqrt{3}+9\chi}} + \frac{9\chi^3\sqrt{3}\operatorname{arccosh}(\frac{1}{2}+\frac{1}{2\chi\sqrt{3}})}{\pi(1+2\chi\sqrt{3})\sqrt{1+2\chi\sqrt{3}-9\chi^2}}, & \chi>0. \end{cases}$$

From these we are able to determine the ground state energies of $\mathcal{H}_{\theta=\pi}$ and $\mathcal{H}_{\theta=0}$,

$$\begin{aligned} E_{\theta=\pi}(\chi_1^+,\chi_1^-) &= -\left[\frac{1}{\pi}+\frac{2\sqrt{3}}{9}\right]\mathcal{L} + \left[\frac{3}{2}-\frac{2\sqrt{3}}{3}\right] + g_{\theta=\pi}(\chi_1^+) + g_{\theta=\pi}(\chi_1^-) + o(\mathcal{L}^0,) \\ E_{\theta=0}(\chi_1^+,\chi_1^-) &= -\left[\frac{1}{2\pi}-\frac{2\sqrt{3}}{9}+\frac{3}{4}\right]\mathcal{L} + \left[-\frac{3}{4}+\frac{2\sqrt{3}}{3}\right] + g_{\theta=0}(\chi_1^+) + g_{\theta=0}(\chi_1^-) + o(\mathcal{L}^0). \end{aligned} \tag{21}$$

In Figure 2 we plot the predicted functions $g_{\theta=\pi}(\chi)$ and $g_{\theta=0}(\chi)$ compared to the equivalent numerical values obtained by solving the the Bethe equations (with $\chi_1^- = \chi_2^{\pm} = 0$).
It is clearly seen that the numerical values match the analytically predicted results even outside of the region $-\frac{1}{3\sqrt{3}} < \chi < \frac{1}{\sqrt{3}}$. We also note that increasing the strength of the boundary field such that it is the dominant term gives the energies associated with the eigenvalues of the boundary operators,

$$\lim_{\chi\to+\infty} g_{\theta=\pi}(\chi) \approx 2\chi \approx \lim_{\chi\to-\infty} g_{\theta=0}(\chi) \qquad \text{and} \qquad \lim_{\chi\to-\infty} g_{\theta=\pi}(\chi) \approx -\chi \approx \lim_{\chi\to+\infty} g_{\theta=0}(\chi).$$

[3]On a technical note, it was observed the magnitude of the boundary Bethe roots will also increase as $\mathcal{L}$ increases for fixed χ. We assume that as $\mathcal{L}$ goes to ∞ the boundary Bethe roots tend to $\pm\infty$ for fixed boundary amplitudes $\chi_k^{\pm}$. This is important when considering the thermodynamical limit.

Figure 2: Numerical values of the functions $g_{\theta=\pi}(\chi)$ and $g_{\theta=0}(\chi)$ obtained via solving the Bethe Equations compared to their predicted analytical expressions for a system of 100 sites. In both plots we have data points for $\chi < -\frac{1}{3\sqrt{3}} \approx -0.193$ and $\chi > \frac{1}{\sqrt{3}} \approx 0.577$.

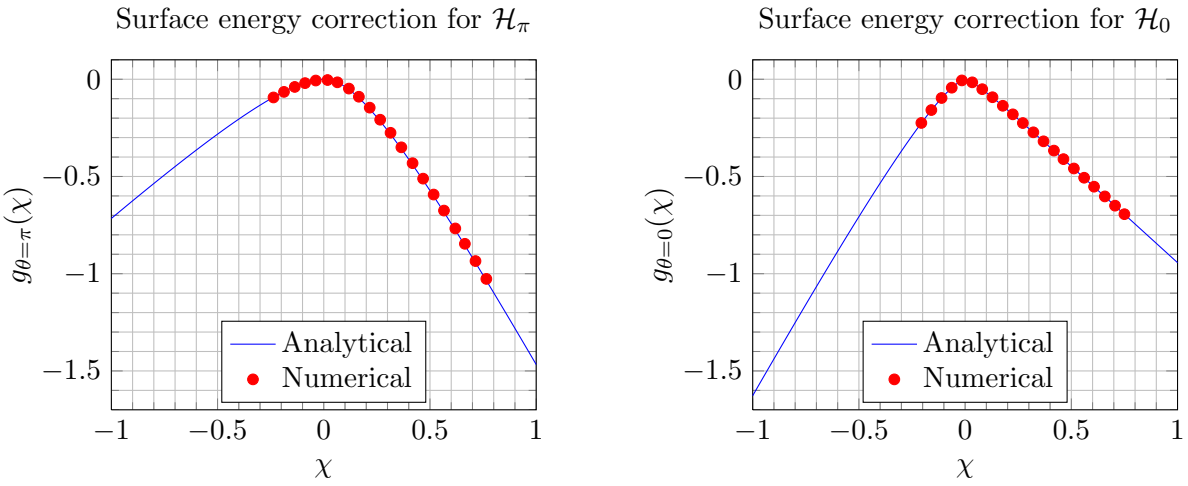

These limits show the correct asymptotic behaviour of the ground state energy, Equations (21), with respect to the χ. This leads us to conjecture that the energies are analytically correct for all values of $\chi_k^\pm \in \mathbb{R}$.

Using Equation (15) along with the relations,

$$E_h^{(k)} = -E_{\theta=\pi}(\chi_k^+, \chi_k^-) \qquad \text{and} \qquad E_l^{(k)} = E_{\theta=0}(\chi_k^+, \chi_k^-),$$

we are able to determine the ground state energy for of $\mathcal{H}_\theta$ for generic θ. We should again recall that we have the constraint $\chi_1^+\chi_2^+ = \chi_1^-\chi_2^- = 0$ and that the interacting boundary terms break the $D(D_3)$ invariance of the model.

4 Excitations and Conformal Field Theories

The presence of a coupling parameter makes the identification of a conformal field theory a difficult takes. Every energy level of the Hamiltonian is dependent on the coupling parameter θ, moreover the energies which are the lowest will change with θ. This implies that model will not be described by a single conformal field theory but rather but multiple ones. To simplify the issue we first study the model at level crossings which turn out to be described by minimal models. This allows us to use powerful machinery and well-known results to accurately describe the model at these points.

To then recover the complete model once all the level crossing have been identified is a relatively straight-forward, albeit non-trivial, task. The main difficulties comes with identifying the previously mentioned pairing rules and connecting them with some conserved quantity of the model. Once all this has been achieved the lowest lying energies will be known for all values of θ.

4.1 Periodic Spin Chain

Here we present an extended version of the results found in the letter [20]. At the level crossings conformal invariance predicts the scaling behaviour of the ground state energy should be

$$E = \epsilon_\infty \mathcal{L} - (c\, v_F) \times \frac{\pi}{6\mathcal{L}} + o(\mathcal{L}^{-1}),$$

where c is the central charge. The operator content of a given realisation of the CFT is constrained by modular invariance of the partition function and boundary conditions [8, 7]. Further constraints are imposed by locality of the physical fields which considered for the complete model, i.e. not at a level crossings. The difference in energy and partial momentum[4] must be of the form,

$$E(\mathcal{L}) - E_0(\mathcal{L}) = \frac{2\pi v_F}{\mathcal{L}} \left(X + n + \bar{n}\right) , \quad P(\mathcal{L}) - P_0(\mathcal{L}) = \frac{2\pi}{\mathcal{L}} \left(s + n - \bar{n}\right) \tag{22}$$

the scaling dimensions $X = h + \bar{h}$ and conformal spins $s = h - \bar{h}$ of the primary fields in the theory can be determined numerically (n, $\bar{n}$ are non-negative integers). To obtain the data numerically we can use solutions to the Bethe equations along with Equations (9) and (11).

4.1.1 Spectrum of $\mathcal{H}_{\theta=\pi}$

It is known that the ground state energy of $\mathcal{H}_\pi$ is given by [2]

$$E_0 \;=\; -\left[\frac{1}{\pi} + \frac{2\sqrt{3}}{9}\right] \mathcal{L} - \frac{12}{5} \times \frac{\pi}{6\mathcal{L}} + o(\mathcal{L}^{-1}) \tag{23}$$

Using the Fermi-velocity we have that the central charge of the effective field theory for the low energy degrees of freedom in $\mathcal{H}_{\theta=\pi}$ is $c = 4/5$: this sector of the model is in the universality class of the minimal model $\mathcal{M}_{(5,6)}$, the conformal weights h, $\bar{h}$ of the primary fields can take the rational values from the Kac table

$$\begin{aligned} h, \bar{h} \;&\in\; \left\{ \frac{(6p-5q)^2 - 1}{120} \,\middle|\, 1 \le q \le p < 5 \right\} \\ &=\; \left\{ 0, \frac{1}{40}, \frac{1}{15}, \frac{1}{8}, \frac{2}{5}, \frac{21}{40}, \frac{2}{3}, \frac{7}{5}, \frac{13}{8}, 3 \right\} \end{aligned}$$

The excitations occurring in this sector for even chain lengths are given in Table 1.
For the states given we have solved the Bethe equations up to a minimum of 40 sites, although in general over 100 sites were considered when possible. As periodicity breaks the $D(D_3)$ invariance of the model we can no longer use the decomposition

$$\pi_{\mathfrak{g}}^{\otimes \mathcal{L}} = \frac{1}{2}(3^{\mathcal{L}-2} + 1)\pi_{\mathfrak{a}} \oplus \frac{1}{2}(3^{\mathcal{L}-2} - 1)\pi_{\mathfrak{b}} \oplus 3^{\mathcal{L}-2} \left[\pi_{\mathfrak{c}} \oplus \pi_{\mathfrak{d}} \oplus \pi_{\mathfrak{e}} \oplus \pi_{\mathfrak{f}}\right],$$

for $\mathcal{L}$ even. However we find by combining some of these irreps we have residual symmetry allowing us to partition the excitations. Specifically the irreps $\pi_{\mathfrak{e}}$ and $\pi_{\mathfrak{f}}$ can not be separated.

[4] At the level crossing there is massive degeneracy and the complete momenta are not unique but partial ones are.

Table 1: Scaling dimensions X_π extrapolated from the finite size behaviour of the ground state and low energy excitations of $\mathcal{H}_{\theta=\pi}$ for even L. $(h,\bar{h})$ are the predictions from the $\mathcal{M}_{(5,6)}$ minimal model. We have also indicated the $D(D_3)$ sector in which the state appears and its degeneracy The operator content of the sector $\pi_{\mathfrak{d}}$ is obtained from that of $\pi_{\mathfrak{c}}$ by interchanging h and $\bar{h}$.

$D(D_3)$	X_π^{num}	$(h,\bar{h})$	spin	degeneracy
$\pi_{\mathfrak{a}} \oplus \pi_{\mathfrak{b}}$	0.000000(1)	$(0,0)$	0	$1 \times 3^{\frac{\mathcal{L}}{2}-1}$
	0.801(3)	$(\frac{2}{5},\frac{2}{5})$	0	$1 \times 3^{\frac{\mathcal{L}}{2}-1}$
	1.80(1)	$(\frac{2}{5},\frac{7}{5}),(\frac{7}{5},\frac{2}{5})$	± 1	$1 \times 3^{\frac{\mathcal{L}}{2}-1}$
$\pi_{\mathfrak{c}}$	0.4668(2)	$(\frac{1}{15},\frac{2}{5})$	$-\frac{1}{3}$	$2 \times 3^{\frac{\mathcal{L}}{2}-1}$
	0.666666(1)	$(\frac{2}{3},0)$	$\frac{2}{3}$	$2 \times 3^{\frac{\mathcal{L}}{2}-1}$
$\pi_{\mathfrak{e}} \oplus \pi_{\mathfrak{f}}$	0.13334(6)	$(\frac{1}{15},\frac{1}{15})$	0	$4 \times 3^{\frac{\mathcal{L}}{2}-1}$
	1.33333(3)	$(\frac{2}{3},\frac{2}{3})$	0	$4 \times 3^{\frac{\mathcal{L}}{2}-1}$

On the other the irreps $\pi_{\mathfrak{a}}$ and $\pi_{\mathfrak{b}}$ can be considered separately but as we have massive degeneracy at $\theta = \pi$ we have the same exponents appearing in both the $\pi_{\mathfrak{a}}$ and $\pi_{\mathfrak{b}}$ sectors, so it is convenient to combine them. The degeneracy of each excitation is also listed in the table. These degeneracies are determined by the symmetry sector, the number of states in that symmetry sector and the pairing multiplicities of those states (which we discuss later). We also classify the different symmetry sectors in terms of Bethe root configurations, in particular the number of roots at $\pm\infty$, summarised in the Table 2. Due to the symmetry of the Bethe equations we can map every Bethe root configuration to another, $\{x_j\} \to \{-x_j\}$. This mapping does not change the symmetry sector for states within $\pi_{\mathfrak{a}} \oplus \pi_{\mathfrak{b}}$ or $\pi_{\mathfrak{e}} \oplus \pi_{\mathfrak{f}}$, but maps states from $\pi_{\mathfrak{c}}$ to $\pi_{\mathfrak{d}}$ and vice-verse. Hence the $(h,\bar{h}) \leftrightarrow (\bar{h},h)$ correspondence between the $\pi_{\mathfrak{c}}$ and $\pi_{\mathfrak{d}}$ sectors.

Table 2: The classification of symmetry sectors in terms of finite and infinite Bethe roots for chains of even length.

Symmetry Sector	$N_- + N_+ + 2N_s$	$n_{-\infty}$	$n_{+\infty}$
$\pi_{\mathfrak{a}} \oplus \pi_{\mathfrak{b}}$	$\mathcal{L}$	0	0
$\pi_{\mathfrak{c}}$	$\mathcal{L}-1$	0	1
$\pi_{\mathfrak{d}}$	$\mathcal{L}-1$	1	0
$\pi_{\mathfrak{e}} \oplus \pi_{\mathfrak{f}}$	$\mathcal{L}-2$	1	1

The excitations appear here for $\mathcal{L}$ even coincide with those from the self-dual ferromagnetic 3-state Potts quantum chain subjected to either periodic of twisted boundary conditions [55]. This stems from both models being constructed from the set of solutions to the star-triangle equation [16], albeit with different limits applied. The excitations in the $\pi_{\mathfrak{a}} \oplus \pi_{\mathfrak{b}}$ and $\pi_{\mathfrak{e}} \oplus \pi_{\mathfrak{f}}$ sectors belong to the periodic 3-state Potts chain and are distinguished by translational properties, where as the excitations in the $\pi_{\mathfrak{c}}$ and $\pi_{\mathfrak{d}}$ sectors correspond to the 3-state Potts chain with twisted boundary conditions allowing for the non-half-integer spins observed. The excitations appearing in the periodic Potts chain have also been determined using Bethe ansatz methods by Albertini et al. [2].

We have also determined the excitations for chains of odd length. In this case the states can

be classified by the eigenvalue of the state under the D_3 rotation operator, σ. The excitations are given Table 3.

Table 3: As Table 1 for odd $\mathcal{L}$. Symmetry is classified by the action of the D_3 rotation σ.

σ	X_π^{num}	$(h, \bar{h})$	spin	degeneracy
1	0.125000(5)	$(0, \frac{1}{8})$	$-\frac{1}{8}$	$1 \times 3^{\frac{\mathcal{L}-1}{2}}$
	0.42502(2)	$(\frac{2}{5}, \frac{1}{40})$	$\frac{3}{8}$	$1 \times 3^{\frac{\mathcal{L}-1}{2}}$
	0.92490(6)	$(\frac{2}{5}, \frac{21}{40})$	$-\frac{1}{8}$	$1 \times 3^{\frac{\mathcal{L}-1}{2}}$
	1.625000(1)	$(0, \frac{13}{8})$	$-\frac{13}{8}$	$1 \times 3^{\frac{\mathcal{L}-1}{2}}$
ω, ω^{-1}	0.091665(2)	$(\frac{1}{15}, \frac{1}{40})$	$\frac{1}{24}$	$2 \times 3^{\frac{\mathcal{L}-1}{2}}$
	0.59168(7)	$(\frac{1}{15}, \frac{21}{40})$	$-\frac{11}{24}$	$2 \times 3^{\frac{\mathcal{L}-1}{2}}$
	0.791667(1)	$(\frac{2}{3}, \frac{1}{8})$	$\frac{13}{24}$	$2 \times 3^{\frac{\mathcal{L}-1}{2}}$

These excitations are not present in the 3-state Potts model since the equivalence to this model is restricted to $\mathcal{L}$ even. We were able to again classify the symmetry sectors in terms of Bethe roots as presented in Table 4. We found that $n_{-\infty} = 0$ in the case of odd length chains.

Table 4: The symmetry sectors classified in terms of finite and infinite Bethe roots for chains of odd length.

Symmetry Sector	$N_- + N_+ + 2N_s$	$n_{-\infty}$	$n_{+\infty}$
1	$\mathcal{L}$	0	0
ω, ω^{-1}	$\mathcal{L} - 1$	0	1

4.1.2 Spectrum of $\mathcal{H}_{\theta=0}$

Using analytical and numerical techniques we found that the ground state energy is,

$$E_0 = -\left[\frac{1}{2\pi} - \frac{2\sqrt{3}}{9} + \frac{3}{4}\right]\mathcal{L} - \frac{3}{2} \times \frac{\pi}{6\mathcal{L}} + o(\mathcal{L}^{-1}) \tag{24}$$

Using the Fermi-velocity we find that the central charge is 1, which does not uniquely define a conformal field theory. The field content of the theory is obtained from the finite size spectrum. One method of determining the the finite size spectrum is using the dressed charge formalism (see appendix) leading to the identification of the Z_4 parafermion theory [58, 26] coinciding with the anti-ferromagnetic 3-state Potts model. The allowed conformal weights for this theory are [26, 42]

$$\begin{aligned} h, \bar{h} &\in \left\{ \frac{l(l+2)}{24} - \frac{m^2}{16} \middle| 0 \le m \le l \le 4,\, l \equiv m \,(\mathrm{mod}\, 2) \right\} \\ &\in \left\{ 0, \frac{1}{16}, \frac{1}{12}, \frac{1}{3}, \frac{9}{16}, \frac{3}{4}, 1 \right\} \end{aligned}$$

Alternately we can solve the Bethe equations directly and determine the scaling behaviour of the low-lying excitations. Here we must consider $\mathcal{L} = 0, 1, 2, 3 \pmod 4$ separately, see Tables 5-7

below. In particular, we find that the finite size gap of the lowest states for $\ell = \mathcal{L} \pmod 4 \neq 0$ is determined by an (anti-)chiral $Z_{k=4}$ spin field with conformal weight $h_\ell = \ell(k-\ell)/(2k(k+2))$.

Table 5: Scaling dimensions X_0 extrapolated from the finite size behaviour of the ground state and low energy excitations of H_0 for $\mathcal{L} = 0 \pmod 4$ (the error of the extrapolation is smaller than the last displayed digit). $(h, \bar{h})$ are the predictions from the Z_4 parafermionic CFT. For the other columns, see Table 1.

$D(D_3)$	X_0^{num}	$(h, \bar{h})$	spin	degeneracy
$\pi_{\mathfrak{a}} \oplus \pi_{\mathfrak{b}}$	0.000000	$(0, 0)$	0	$1 \times 3^{\frac{\mathcal{L}}{2}-1}$
$\pi_{\mathfrak{c}}$	0.333332	$(0, \frac{1}{3})$	$-\frac{1}{3}$	$2 \times 3^{\frac{\mathcal{L}}{2}-1}$
$\pi_{\mathfrak{e}} \oplus \pi_{\mathfrak{f}}$	0.166667	$(\frac{1}{12}, \frac{1}{12})$	0	$4 \times 3^{\frac{\mathcal{L}}{2}-1}$
	0.666667	$(\frac{1}{3}, \frac{1}{3})$	0	$4 \times 3^{\frac{\mathcal{L}}{2}-1}$

Table 6: As Table 5 for $\mathcal{L} = 1 \pmod 4$. The excitations for chains with length $\mathcal{L} = 3 \pmod 4$ have the same exponents but the opposite spin. Symmetry is classified by the action of the D_3 rotation σ.

σ	X_0^{num}	$(h, \bar{h})$	spin	degeneracy
1	0.062500	$(\frac{1}{16}, 0)$	$\frac{1}{16}$	$1 \times 3^{\frac{\mathcal{L}-1}{2}}$
	0.562500	$(\frac{9}{16}, 0)$	$\frac{9}{16}$	$1 \times 3^{\frac{\mathcal{L}-1}{2}}$
	0.812500	$(\frac{1}{16}, \frac{3}{4})$	$-\frac{11}{16}$	$1 \times 3^{\frac{\mathcal{L}-1}{2}}$
ω, ω^{-1}	0.145833	$(\frac{1}{16}, \frac{1}{12})$	$-\frac{1}{48}$	$2 \times 3^{\frac{\mathcal{L}-1}{2}}$
	0.395833	$(\frac{1}{16}, \frac{1}{3})$	$-\frac{13}{48}$	$2 \times 3^{\frac{\mathcal{L}-1}{2}}$
	0.645833	$(\frac{9}{16}, \frac{1}{12})$	$\frac{23}{48}$	$2 \times 3^{\frac{\mathcal{L}-1}{2}}$

Table 7: As Table 5 but for $\mathcal{L} = 2 \pmod 4$.

$D(D_3)$	X_0^{num}	$(h, \bar{h})$	spin	degeneracy
$\pi_{\mathfrak{a}} \oplus \pi_{\mathfrak{b}}$	0.750000	$(0, \frac{3}{4}) \times 2$, $(\frac{3}{4}, 0) \times 2$	$\pm\frac{3}{4}$	$1 \times 3^{\frac{\mathcal{L}}{2}-1}$
$\pi_{\mathfrak{c}}$	0.083333	$(0, \frac{1}{12})$	$-\frac{1}{12}$	$2 \times 3^{\frac{\mathcal{L}}{2}-1}$
	1.083333	$(\frac{3}{4}, \frac{1}{3})$	$\frac{5}{12}$	$2 \times 3^{\frac{\mathcal{L}}{2}-1}$
$\pi_{\mathfrak{e}} \oplus \pi_{\mathfrak{f}}$	0.416667	$(\frac{1}{12}, \frac{1}{3}), (\frac{1}{3}, \frac{1}{12})$	$\pm\frac{1}{4}$	$4 \times 3^{\frac{\mathcal{L}}{2}-1}$

As with the previous case we again can partition the excitations in into residual symmetry sectors. These sectors are still characterised by the number of Bethe roots at $\pm\infty$ as described in Table 2.

Comparing these excitation to the anti-ferromagnetic 3-state Potts chain [2, 42] (for $\mathcal{L}$ even), we find that the excitations in the $\pi_{\mathfrak{a}} \oplus \pi_{\mathfrak{b}}$ and $\pi_{\mathfrak{e}} \oplus \pi_{\mathfrak{f}}$ were previously identified and restricted to the $n_{+\infty} = n_{-\infty}$ case. We were unable to find any literature dealing with this end of the twisted 3-Potts model, however, we expect that the excitations in that case to match those

appearing in the $\pi_{\mathfrak{c}}$ and $\pi_{\mathfrak{d}}$ sectors. Similarly the excitations for odd $\mathcal{L}$ have not previously been studied.

4.1.3 Pairing rules and discussion

Through studying the two above cases of $\theta = 0, \pi$ we are able to deduce the behaviour for all the level crossings, i.e. when θ is a multiple of $\frac{\pi}{2}$, as the energy spectra of $\mathcal{H}^{(1)}$ and $\mathcal{H}^{(2)}$ are identical, although the momenta are of opposite sign. The analysis of the model is extended to generic θ by determining pairing rules. Since the symmetry sectors identified above refer to the complete system two levels of $\mathcal{H}^{(1)}$, $\mathcal{H}^{(2)}$ can pair if and only if[5] they belong to the same symmetry sectors[6] [21]. Pairing is uniform within symmetry sectors (shown in Table 8) and can be used along with Equations (9,11,23,24) to determine the complete energy. The pairing of levels also ensures the locality of the physical fields by restricting spins to either whole-, half- or quarter-integer. For example, for $\mathcal{L} = 0 \pmod 4$ with $\theta = \frac{3\pi}{4}$ we find the excitations $(\frac{1}{15}, \frac{2}{5})$ from $\mathcal{H}_\pi$ and $(0, \frac{1}{12})$ from $H_{\frac{\pi}{2}}$ (same spectrum as $\mathcal{H}_0$) both belong to the $\pi_{\mathfrak{c}}$ symmetry sector, thus they pair together twice and have a spin of $\frac{-1}{3} - \frac{-1}{12} = \frac{-1}{4}$.

Table 8: The pairing multiplicities, m_p, of the periodic spin chain for any two energies of $\mathcal{H}^{(1)}$ and $\mathcal{H}^{(2)}$ that belong to the same symmetry sector. If the energies do not belong to the same symmetry sector then they do not pair, i.e. the pairing multiplicity is zero.

	$\mathcal{L} = 0 \pmod 2$				$\mathcal{L} = 1 \pmod 2$	
Sector	$\pi_{\mathfrak{a}} \oplus \pi_{\mathfrak{b}}$	$\pi_{\mathfrak{c}}$	$\pi_{\mathfrak{d}}$	$\pi_{\mathfrak{e}} \oplus \pi_{\mathfrak{f}}$	1	w, w^{-1}
m_p	1	2	2	4	1	2

The complete model can be summarised by Figure 3.

4.2 Periodic Fusion Path Chain

By construction this chain must share bulk properties with the periodic spin chain of the previous section, including energy per unit lattice site, Fermi velocity and central charge. Furthermore we find that many of the energies appearing in the periodic fusion path chain are also present in the periodic spin chain. Specifically, these are the energies in the $\pi_{\mathfrak{a}} \oplus \pi_{\mathfrak{b}}$ and $\pi_{\mathfrak{e}} \oplus \pi_{\mathfrak{f}}$ symmetry sectors and are numerically exact[7]. However the degeneracies of the identical energies in the two formalisms do not match. Amongst the energies appearing in both are the the ground states, when realised, given by Equations (23) and (24) for $\mathcal{H}_\pi$ and $\mathcal{H}_0$, respectively.

4.2.1 Spectrum of $\tilde{\mathcal{H}}_{\theta=\pi}$

We are still in the $M_{(5,6)}$ universality class ($c = \frac{4}{5}$). Using numerical methods we find the excitations as given in Table 9.

[5] More accurately, the *only if* direction is true because of the symmetry sectors being a property of the complete model while the *if* direction has been observed to be true.

[6] If an excitation $(h, \bar{h})$ of $\pm\mathcal{H}^{(1)}$ belongs to a certain symmetry sector then the corresponding excitation $(h, \bar{h})$ of $\pm\mathcal{H}^{(2)}$ will belong to the same symmetry sector. We will later see this is not the case for the braided and open chains.

[7] At least up to system sizes of $\mathcal{L} = 10$. Systems with longer chain lengths were not numerically computed.

Figure 3: Conformal field theory description of the periodic integrable $D(D_3)$ symmetric model for generic θ. Level crossing are described by minimal models, either Z_4 parafermions or $\mathcal{M}_{(5,6)}$, while the regions in between are described by a product of the theories of the two adjacent level crossings. Therefore regions I and IV correspond to a $Z_4 \otimes \mathcal{M}_{(5,6)}$ theory, while regions II and III correspond respectively to $Z_4 \otimes Z_4$ and $\mathcal{M}_{(5,6)} \otimes \mathcal{M}_{(5,6)}$ theories.

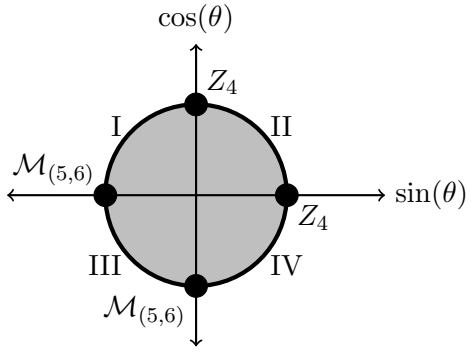

For energy levels appearing in both formalisms we have used the numerical Bethe ansatz results from the previous section to determine the exponent, while for the new energy levels we have used data from the numerical diagonalisation of the Hamiltonian for chains sizes up to 10 sites. The new excitations appearing in this chain also do not correspond to excitations of the 3-state Potts chains subject to the boundary conditions previously studied [55]. Moreover because the formulation of this chain is reliant on $D(D_3)$ symmetry, which is not present in the usual 3-state Potts local Hamiltonian, it is reasonable to expect that these excitations won't appear for any formulation of the 3-state Potts model. The periodicity of the chain also breaks the $D(D_3)$ invariance of the model [19] and we are unable assign symmetry sectors to the excitations as we did before.

4.2.2 Spectrum of $\tilde{\mathcal{H}}_{\theta=0}$

Using numerical methods we can find the excitations of the occurring for the Hamiltonian $\mathcal{H}_{\theta=0}$. This is done for even $\mathcal{L}$ and split according to if $\frac{\mathcal{L}}{2}$ is even or odd. The excitations are,

$$(h,\bar{h}) \in \begin{cases} \left\{(0,0),(\frac{1}{16},\frac{1}{16})^\star,(\frac{1}{12},\frac{1}{12}),(\frac{1}{3},\frac{1}{3})\right\}, & \mathcal{L} \equiv 0 \bmod 4, \\ \left\{(\frac{1}{16},\frac{1}{16})^\star,(0,\frac{3}{4}),(\frac{3}{4},0),(\frac{1}{3},\frac{1}{12}),(\frac{1}{12},\frac{1}{3})\right\}, & \mathcal{L} \equiv 2 \bmod 4, \end{cases}$$

where we have again have used a $\star$ to denote new excitations. As the spectra need to be considered differently for $\frac{\mathcal{L}}{2}$ odd and even, we have effectively split our number of data points for each excitation. Thus the accuracy here is lower than the excitations for $\mathcal{H}_{\theta=\pi}$.

4.2.3 Pairing rules and discussion

In contrast to the periodic spin formulation the pairing rules for the periodic fusion path chain are not of a simple form. Pairing is no longer transitive implying the pairing table would have no block structure. Additionally the symmetry sectors used to describe the periodic spin chain can not be used to describe this case as the periodic closure of the fusion path chain breaks

Table 9: Scaling dimensions X_π extrapolated from the finite size behaviour of the ground state and low energy excitations of $\mathcal{H}_\pi$ for $\mathcal{L} = 0 \pmod 2$. The values with a $\star$ correspond to exponents not appearing the periodic spin formulation and therefore also not in the 3-state Potts model. Scaling dimensions marked with a ‡ have no estimation of uncertainty due to a lack of data points. Each combination of $(h, \bar{h})$ appearing in the second column has the degeneracy given in the last column.

$X_{\text{approx.}}$	$(h, \bar{h})$	spin	degeneracy
0.000000(1)	$(0, 0)$	0	$\frac{1}{2}(3^{\frac{\mathcal{L}}{2}} + 1)$
$0.051(3)^\star$	$(\frac{1}{40}, \frac{1}{40})$	0	$\frac{1}{2}(3^{\frac{\mathcal{L}}{2}} + 1)$
0.13334(4)	$(\frac{1}{15}, \frac{1}{15})$	0	$3^{\frac{\mathcal{L}}{2}}$
$0.250(1)^\star$	$(\frac{1}{8}, \frac{1}{8})$	0	$\frac{1}{2}(3^{\frac{\mathcal{L}}{2}} + 1)$
$0.56(-)^{\star\ddagger}$	$(\frac{1}{40}, \frac{21}{40}), (\frac{21}{40}, \frac{1}{40})$	$\pm\frac{1}{2}$	$\frac{1}{2}(3^{\frac{\mathcal{L}}{2}} - 1)$
0.801(3)	$(\frac{2}{5}, \frac{2}{5})$	0	$\frac{1}{2}(3^{\frac{\mathcal{L}}{2}} + 1)$
$1.06(-)^{\star\ddagger}$	$(\frac{21}{40}, \frac{21}{40})$	0	$\frac{1}{2}(3^{\frac{\mathcal{L}}{2}} + 1)$
1.33333(3)	$(\frac{2}{3}, \frac{2}{3})$	0	$3^{\frac{\mathcal{L}}{2}}$
1.80(1)	$(\frac{2}{5}, \frac{7}{5}), (\frac{7}{5}, \frac{2}{5})$	± 1	$\frac{1}{2}(3^{\frac{\mathcal{L}}{2}} - 1)$

the $D(D_3)$ symmetry in the spin sense. However, for the anyon model it is possible to define a conserved topological charged bases of the $D(D_3)$ F-moves aforementioned [17, 27]. The different topological sectors are labelled by the irreps in the decomposition of $\pi_{\mathfrak{g}}^{\otimes\mathcal{L}}$. A better understanding of these topological symmetry sectors may lead to insight into the pairing rules.

The identification of the excitations has utilised techniques which numerically diagonalise the Hamiltonian. This is clearly limited by computational power. As the periodic fusion path chain shares energies with the periodic spin chain we have confidence in the ones we have successfully identified. However, the excitations which are do not appear in the periodic spin chain are difficult to determine within any great accuracy. To ensure that we have identified all excitations of the level crossings and answer the open problems associated with this model, such as pairing rules, more advanced techniques would be required such as using integrability reliant techniques associated with RSOS models or utilising better numerical methods for the diagonalisation of Hamiltonian.

4.3 Braided Chain

4.3.1 Spectrum of $\mathcal{H}_{\theta=\pi}$

The full spectrum of the $\mathcal{H}_{\theta=\pi}$ braided chain is a subset of the spectrum of the $\mathcal{H}_{\theta=\pi}$ periodic spin chain. In particular we find that the energies present are those that appeared in the symmetry sectors $\pi_{\mathfrak{a}} \oplus \pi_{\mathfrak{b}}$ and $\pi_{\mathfrak{c}}$ of the periodic chain for even $\mathcal{L}$ and in the $\sigma = 1$ for odd $\mathcal{L}$. This corresponds to Bethe root configurations with $n_{-\infty} = 0$. Therefore the low-lying excitations for this chain correspond to the pairs of conformal weights,

$$(h, \bar{h}) \quad \in \quad \begin{cases} \left\{(0,0), (\frac{2}{5}, \frac{2}{5}), (\frac{2}{5}, \frac{7}{5}), (\frac{7}{5}, \frac{2}{5}), (\frac{1}{15}, \frac{2}{5}), (\frac{2}{3}, 0)\right\}, & \mathcal{L} \quad \text{even}, \\ \left\{(0, \frac{1}{8}), (\frac{2}{5}, \frac{1}{40}), (\frac{2}{5}, \frac{21}{40}), (0, \frac{13}{8})\right\}, & \mathcal{L} \quad \text{odd}. \end{cases}$$

The braided chain has the full $D(D_3)$ symmetry implying we could classify excitations in terms of the irreps, however, we find that because of the difference in global symmetry we now have

energies appearing across multiple symmetry sectors. We also remark that since there are less excitations each of them has a higher degeneracy than the same excitation in the periodic chain. For chains of even length the degeneracies are now either $3\times 3^{\frac{\mathcal{L}}{2}-1}$ or $6\times 3^{\frac{\mathcal{L}}{2}-1}$ depending on which symmetry sectors they are in. While for chains of odd length every excitation has degeneracy $3\times 3^{\frac{\mathcal{L}-1}{2}}$.

4.3.2 Spectrum of $\mathcal{H}_{\theta=0}$

As $\mathcal{H}_{\theta=0}=-\mathcal{H}_{\theta=\pi}$ we again have the excitations appearing also were identified in the periodic section. The ones that appear are,

$$(h,\bar{h})\in\begin{cases}\left\{(0,0),(0,\frac{1}{3})\right\}, & \mathcal{L}\equiv 0 \bmod 4,\\ \left\{(0,\frac{3}{4}),(\frac{3}{4},0),(0,\frac{1}{12}),(\frac{3}{4},\frac{1}{3})\right\}, & \mathcal{L}\equiv 1 \bmod 4,\\ \left\{(\frac{1}{16},0),(\frac{9}{16},0),(\frac{1}{16},\frac{3}{4})\right\}, & \mathcal{L}\equiv 2 \bmod 4,\\ \left\{(0,\frac{3}{4}),(\frac{3}{4},0),(\frac{1}{12},0),(\frac{1}{3},\frac{3}{4})\right\}, & \mathcal{L}\equiv 3 \bmod 4.\end{cases}$$

4.3.3 Pairing rules and discussion

Like the periodic case by studying the braided chain at $\theta=0,\pi$ we can extrapolate finite size data to determine the behaviour at all of the level crossings. We observe important differences between the periodic and braided models. We find that an energy of $\mathcal{H}^{(1)}$ will appear in multiple symmetry sectors and similarly for the energies of $\mathcal{H}^{(2)}$. However, we observe that for a specific exciation, $(h,\bar{h})$, the symmetry sectors it appears in for $\theta=0,\pi$ are not necessarily the same as the ones it appears in for $\theta=\frac{\pi}{2},\frac{3\pi}{2}$. Excitations appear in multiple symmetry sectors in such a way that every two levels pair. For $\pi<\theta<\frac{3\pi}{2}$ and $\mathcal{L}$ even we construct the pairing table (Table 10) of the lowest excitations. In this table we can clearly see excitations of $\mathcal{H}_{\theta=\pi}$ and $\mathcal{H}_{\theta=\frac{3\pi}{2}}$ appearing in multiple symmetry sectors in such a way that every excitation pairs with all others. We should also remark that we could have formulated this in the fusion path basis which would have provided an equivalent model up to degeneracies.

Table 10: Pairing table for the lowest excitations of the periodic spin chain for $\pi<\theta<\frac{3\pi}{2}$.

$X_{\theta=\frac{3\pi}{2}}$ \ $X_{\theta=\pi}$	$(0,0)$ $(\frac{2}{5},\frac{2}{5})$ $(\frac{2}{5},\frac{7}{5})$ $(\frac{7}{5},\frac{2}{5})$	$(\frac{1}{15},\frac{2}{5})$ $(\frac{2}{3},0)$
$(0,0)$ $(\frac{2}{5},\frac{2}{5})$ $(\frac{2}{5},\frac{7}{5})$ $(\frac{7}{5},\frac{2}{5})$	$m_p=1$ $\pi_{\mathfrak{a}}\oplus\pi_{\mathfrak{b}}$	$m_p=2$ $\pi_{\mathfrak{c}}$
$(\frac{1}{15},\frac{2}{5})$ $(\frac{2}{3},0)$	$m_p=2$ $\pi_{\mathfrak{d}}$	$m_p=4$ $\pi_{\mathfrak{e}}\oplus\pi_{\mathfrak{f}}$

4.4 Open Chain

We now consider the open chain. At level crossings conformal invariance predicts that the lowest energies of the open chain with free ends, i.e. $\chi_1^{\pm}=\chi_2^{\pm}=0$, have the scaling behaviour

given by

$$E = \epsilon_\infty \mathcal{L} + f_0 + \frac{\pi v_F}{\mathcal{L}} \left(-\frac{c}{24} + h + n \right) + o(\mathcal{L}^{-1}),$$

where c is the central charge, v_F is the Fermi-velocity, h is a conformal weight and n is a non-negative integer.

4.4.1 Spectrum of $\mathcal{H}_{\theta=\pi}$

The ground state ($h = 0$) energy is,

$$E_0 = -\left[\frac{1}{\pi} + \frac{2\sqrt{3}}{9}\right]\mathcal{L} + \left[\frac{3}{2} - \frac{2\sqrt{3}}{3}\right] - \frac{12}{5} \times \frac{\pi}{24\mathcal{L}} + o(\mathcal{L}^{-1}).$$

As is the case with the periodic chain we have that $v_F = 3$ and $c = \frac{4}{5}$, yielding the same CFT as expected. From our numerical solutions to the Bethe ansatz equations we found the lowest energies corresponded to conformal weights

$$h \in \begin{cases} \left\{0, \frac{2}{3}\right\}, & \mathcal{L}\,\text{even}, \\ \left\{\frac{1}{8}, \frac{13}{8}\right\}, & \mathcal{L}\,\text{odd}. \end{cases}$$

and descendants thereof.

4.4.2 Spectrum of $\mathcal{H}_{\theta=0}$

The ground state of the open chain for $\theta = 0$ is,

$$E_0 = -\left[\frac{1}{2\pi} - \frac{2\sqrt{3}}{9} + \frac{3}{4}\right]\mathcal{L} + \left[-\frac{3}{4} + \frac{2\sqrt{3}}{3}\right] - \frac{3}{2} \times \frac{\pi}{24\mathcal{L}} + o(\mathcal{L}^{-1}),$$

which gives $v_F = \frac{3}{2}$ and $c = 1$, in agreement with the periodic chain. Numerical data showed that the lowest excitations appearing correspond to the conformal weights

$$(h, \bar{h}) \in \begin{cases} \left\{0, \frac{1}{3}, 1\right\}, & \mathcal{L} \equiv 0 \bmod 4, \\ \left\{\frac{1}{16}, \frac{9}{16}\right\}, & \mathcal{L} \equiv 1 \bmod 4, \\ \left\{\frac{1}{12}, \frac{3}{4}(\times 2)\right\}, & \mathcal{L} \equiv 2 \bmod 4, \\ \left\{\frac{1}{16}, \frac{9}{16}\right\}, & \mathcal{L} \equiv 3 \bmod 4. \end{cases}$$

along with some their descendants.

4.4.3 Pairing rules and discussion

This model, like the braided version, has the full global symmetry of the algebra $D(D_3)$ and also has all energies pairing.

5 Discussion

In this paper we have analysed the low energy spectrum of the integrable $D(D_3)$ symmetric chain subject to various boundary conditions. In the spin chain formulation the Hamiltonian derives from a commuting two-parameter transfer matrix of a vertex model and the eigenvalues

can be obtained by Bethe ansatz methods. We have constructed a related class of models with local $D(D_3)$ symmetry using the fusion path formulation: these models, too, are integrable as they can be obtained from a solution to the Yang-Baxter equation for a face (or RSOS) model. For open and braided boundary conditions the two formulations of the model are equivalent. For periodic closure, however, the fusion path chain differs from the spin chain by boundary terms.

Based on our analysis of the spectrum of these models we have identified the conformal field theories providing an effective description of the low energy modes to contain two sectors from – depending on the parameter θ – the minimal model $\mathcal{M}_{(5,6)}$ (the three-state Potts model) and the Z_4 parafermion. The physical fields are products of operators from these sectors. The individual factors can carry fractional (non-integer or non-(para)fermionic) spins implying the appearance of Virasoro characters in the partition function of the model which have not been discussed in the context of $\mathcal{M}_{(5,6)}$ or Z_4 alone.

The locality of physical fields in the model is guaranteed by pairing rules. This situation is similar to other models with several gapless modes propagating with different Fermi velocities [6, 23, 24]. We have to emphasise, however, that in the present models this factorisation of different modes is *exact* already for finite chains and on all energy scales, unlike in say the separation of spin and charge degrees of freedom observed within the low energy spectrum of the one-dimensional Hubbard model where the coupling between the sectors becomes manifest in subleading corrections to scaling. Another difference for the model studied here is that the two sectors of the effective theory are not related to subalgebras of the global symmetry of the model. Therefore, to establish the pairing rules and corresponding multiplicities we have resorted to numerical studies of small systems together with counting arguments for the total number of states of the system. For the spin chain formulation we found that the pairing is determined the boundary conditions and can be related to the residual symmetry of a given eigenstate. It is also reflected by the appearance of infinite roots appearing in the configurations solving the Bethe equations of the model. The spectrum of the periodic $D(D_3)$ model in the fusion path formulation also shows pairing on all energy scales. Unlike in the spin chain formulation, however, the pairing is not transitive and cannot be described based on residual symmetries as in the spin chain. The determining of the pairing rules and as to whether these rules are connected to topological invariants involving the $D(D_3)$ F-moves is an interesting open problem of this model.

As a first step, numerical methods could be used to form conjectures. Ultimately, however, it would be desirable to obtain the complete picture starting from the integrable structures underlying this model. Apart from the understanding of pairing rules this concerns in particular the solution of the spectral problem of the anyon chain: the fact that the two formulations of the periodic chain have exponentially (in system size) many energies in common suggests that there should exist a formulation of the eigenvalue problem in terms of Bethe type equations for the fusion path chain. We shall address this problem in future work.

Acknowledgements

The authors would like to thank Jesper Romers for providing mathematica code that generated the F-moves for the $D(D_3)$ anyons, along with Karen Dancer, Fabian Essler. Jon Links and Robert Weston for discussing various topics relating to this article and referring the authors to relevant literature.

Parts of the numerical data used in this work have been obtained using the RRZN cluster

system at Leibniz Universitt Hannover. Support for this project by the Deutsche Forschungsgemeinschaft is gratefully acknowledged.

References

[1] G. Albertini, S. Dasmahapatra and B.M. McCoy, *Spectrum and completeness of the integrable 3-state Potts model: a finite size study*, Int. J. Mod. Phys. A, **7, Suppl. 1A**, 1-53, (1992).

[2] G. Albertini, S. Dasmahapatra and B.M. McCoy, *Spectrum doubling and the extended Brillouin zone in the excitations of the three state Potts spin chain*, Phys. Lett. A, **170**, 397-403, (1992).

[3] F.C. Alcaraz, M.N. Barber and M.T. Batchelor, *Conformal invariance, the XXZ chain and the operator content of two-dimensional critical systems*, Ann. Phys. (NY), **182**, 280-343, (1988).

[4] E. Ardonne, J. Gukelberger, A.W.W. Ludwig, S. Trebst and M. Troyer, *Microscopic models of interacting Yang-Lee anyons*, New J. Phys., **13**, 045006, (2011).

[5] L. Balents, M.P.A. Fisher and S.M. Girvin, *Fractionalization in an easy-axis Kagome antiferromagnet*, Phys. Rev. B, **65**, 224412, (2002).

[6] N.M. Bogoliubov, A.G. Izergin and V.E. Korepin, *Critical exponents for integrable models*, Nucl. Phys. B, **275 [FS17]**, 687-705, (1986).

[7] A. Cappelli, C. Itzykson and J.B. Zuber, *Modular invariant partition functions in two dimensions*, Nucl. Phys. B, **280 [FS18]**, 445-465, (1987).

[8] J.L. Cardy, *Effect of boundary conditions on the operator content of two-dimensional conformally invariant theories*, Nucl. Phys. B, **275**, 200-218, (1986).

[9] V. Chari and A. Pressley, *A guide to quantum groups*, Cambridge University Press, (1994).

[10] K.A. Dancer, P.E. Finch, P.S. Isaac and J. Links, *Integrable boundary conditions for a non-Abelian anyon chain with $D(D_3)$ symmetry*, Nucl. Phys. B, **812**, 456–469, (2009).

[11] K.A. Dancer, P.S. Isaac and J. Links, *Representations of the quantum double of finite group algebras and spectral parameter dependent solutions of the Yang–Baxter equation*, J. Math. Phys., **47**, 103511, (2006).

[12] M. de Wild Propitius and F.A. Bais, *Discrete gauge theories*, In Particles and Fields, Eds. G. Semenoff and L. Vinet, CRM Series in Mathematical Physics (Springer-Verlag, New York), 353–353, (1998).

[13] P. Di Francesco and J.B. Zuber, SU(N) *lattice integrable models associated with graphs*, Nuclear Phys. B, **338**, 602–646, (1990).

[14] R. Dijkgraaf, V. Pasquier and P. Roche, *Quasi Hopf algebras, group cohomology and orbifold models*, Nucl. Phys. (Proc. Supp.), **18**, 60–72, (1990).

[15] F. Essler, H. Frahm, F. Göhmann, A. Klümper and V.E. Korepin, *The one-dimensional Hubbard model*, Cambridge University Press, (2005).

[16] V.A. Fateev and A.B. Zamolodchikov, *Self-dual solutions of the star-triangle relation in $\mathbb{Z}_N$-Models*, Phys. Lett. A, **92**, 37–39, (1982).

[17] A. Feiguin, S. Trebst, A.W.W. Ludwig, M. Troyer, A.Y. Kitaev, Z. Wang and M.H. Freedman, *Interacting Anyons in Topological Quantum Liquids: The Golden Chain*, Physical Review Letters, **98**, 160409, (2007).

[18] P.E. Finch, *Integrable Hamiltonians with $D(D_n)$ symmetry from the Fateev-Zamolodchikov model*, J. Stat. Mech., P04012, (2011).

[19] P.E. Finch, *From spin to anyon notation: The XXZ Heisenberg model as a D_3 (or $su(2)_4$) anyon chain*, arXiv:1201.4470, (2012).

[20] P.E. Finch and H. Frahm, *Collective states of interacting $D(D_3)$ non-Abelian anyons*, J. Stat. Mech., **5**, L05001, (2012).

[21] P.E. Finch, H. Frahm and J. Links, *Ground-state phase diagram for a system of interacting, $D(D_3)$ non-Abelian anyons*, Nucl. Phys. B, **844**, 129–145, (2011).

[22] A. Foerster, *Quantum group invariant supersymmetric t-J model with periodic boundary conditions*, J. Phys. A, **29**, 7625–7633, (1996).

[23] H. Frahm and V.E. Korepin, *Critical exponents for the one-dimensional Hubbard model*, Phys. Rev. B, **42**, 10553-10565, (1990).

[24] H. Frahm and N.C. Yu, *Finite size effects in the integrable XXZ Heisenberg model with arbitrary spin*, J. Phys. A, **23**, 2115, (1990).

[25] D. Gepner, *Foundations of Rational Quantum Field Theory, I*, Caltech preprint CALT-68-1825, arXiv:hep-th/9211100, (1992).

[26] D. Gepner and Z. Qiu, *Modular invariant partition functions for parafermionic field theories*, Nucl. Phys. B, **285**, 423-453, (1987).

[27] C. Gils, E. Ardonne, S. Trebst, D.A. Huse, A.W.W. Ludwig, M. Troyer and Z. Wang, *Anyonic quantum spin chains: Spin-1 generalizations and topological stability*, (in preperation), (2012).

[28] C. Gils, E. Ardonne, S. Trebst, A. Ludwig, M. Troyer and Z. Wang, *Collective States of Interacting Anyons, Edge States, and the Nucleation of Topological Liquids*, Phys. Rev. Lett., **103**, 070401, (2009).

[29] C. Gómez, M. Ruiz-Altaba and G. Sierra, *Quantum groups in two-dimensional physics*, Cambridge University Press, (1996).

[30] M.D. Gould, *Quantum double finite group algebras and their representations*, Bull. Aust. Math. Soc., **48**, 275–301, (1993).

[31] H. Grosse, S. Pallua, P. Prester and E. Raschhofer, *On a quantum group invariant spin chain with non-local boundary conditions*, J. Phys. A: Math. Gen., **27**, 4761-4771, (1994).

[32] Y. Ikhlef, J.L. Jacobsen and H. Saleur, *A Temperley-Lieb quantum chain with two- and three-site interactions*, J. Phys. A, **42**, 292002, (2009).

[33] P. Kakashvili and E. Ardonne, *Integrability in anyonic quantum spin chains via a composite height model*, Phys. Rev. B, **85**, 115116, (2012).

[34] M. Karowski and A. Zapletal, *Quantum Group Invariant Integrable n-State Vertex Models with Periodic Boundary Conditions*, Nucl. Phys. B, **419**, 567-588, (1994).

[35] A. Kitaev, *Anyons in an exactly solved model and beyond*, Ann. Phys., **321**, 2–111, (2006).

[36] A.Yu. Kitaev, *Fault-tolerant quantum computation by anyons*, Ann. Phys. (NY), **303**, 2-30, (2003).

[37] N. Kitanine, K.K. Kozlowski, J.M. Maillet, N.A. Slavnov and V. Terras, *A form factor approach to the asymptotic behavior of correlation functions in critical models*, J. Stat. Mech., P12010, (2011).

[38] V.E. Korepin, N.M. Bogoliubov and A.G. Izergin, *Quantum inverse scattering method and correlation functions*, Cambridge University Press, (1993).

[39] R.B. Laughlin, *Anomalous quantum Hall effect: an incompressible quantum fluid with fractionally charged excitations*, Phys. Rev. Lett., **50**, 1395, (1983).

[40] A.W. Ludwig, D. Poilblanc, S. Trebst and M. Troyer, *Two-dimensional quantum liquids from interacting non-Abelian anyons*, New J. Phys., **13**, 045014, (2011).

[41] S. Majid, *Foundations of quantum group theory*, Cambrigde University Press, (1995).

[42] B.M. McCoy and R. Kedem, *Construction of modular branching functions from Bethe's equations in the 3-state Potts chain*, J. Stat. Phys, **17**, 865, (1993).

[43] J. McKay, *Graphs, singularities, and finite groups*, The Santa Cruz Conference on Finite Groups (Univ. California, Santa Cruz, Calif., 1979), **37**, 183–186, (1980).

[44] R. Moessner and S.L. Sondhi, *Resonating valence bond phase in the triangular lattice quantum dimer model*, Phys. Rev. Lett., **86**, 1881, (2001).

[45] G. Moore and N. Read, *Nonabelions in the fractional quantum Hall effect*, Nucl. Phys. B, **360**, 362–396, (1991).

[46] C. Nayak, S.H. Simon, A. Stern, M. Freedman and S.D. Sarma, *Non-Abelian Anyons and Topological Quantum Computation*, Rev. Mod. Phys., **80**, 1083-1159, (2008).

[47] V. Pasquier, *Lattice derivation of modular invariant partition functions on the torus*, J. Phys. A, **20**, L1229–L1237, (1987).

[48] V. Pasquier, *Two-Dimensional Critical Systems Labelled by Dynkin Diagrams*, Nucl. Phys. B, **285**, 162–172, (1987).

[49] V. Pasquier, *Etiology of IRF models*, Comm. Math. Phys., **118**, 355–364, (1988).

[50] P. Roche, *On the construction of integrable dilute ADE models*, Physics Letters B, **285**, 49-53, (1992).

[51] E.K. Sklyanin, *Boundary conditions for integrable quantum systems*, J. Phys. A: Math. Gen., **21**, 2375-2389, (1988).

[52] J. Suzuki, *Simple excitations in the nested Bethe-ansatz model*, J. Phys. A: Math. Gen., **21**, L1175–L1180, (1988).

[53] S. Trebst, E. Ardonne, A. Feiguin, D. Huse, A. Ludwig and M. Troyer, *Collective states of interacting Fibonacci anyons*, Phys. Rev. Lett., **101**, 050401, (2008).

[54] S. Trebst, M. Troyer, Z. Wang and A.W.W. Ludwig, *A short introduction to Fibonacci anyon models*, Prog. Theor. Phys. Suppl., **176**, 384, (2008).

[55] G. von Gehlen and V. Rittenberg, *Operator content of the three-state Potts quantum chain,*, J. Phys. A: Math. Gen., **19**, L625, (1986).

[56] S.O. Warnaar and B. Nienhuis, *Solvable lattice models labelled by Dynkin diagrams*, J. Phys. A, **26**, 2301–2316, (1993).

[57] C.N. Yang and C.P. Yang, *Thermodynamics of a one-dimensional system of bosons with repulsive delta-function interaction*, J. Math. Phys., **10**, 1115-1122, (1969).

[58] A.B. Zamolodchikov and V.A. Fateev, *Nonlocal (parafermion) currents in two-dimensional conformal quantum field theory and self-dual critical points in Z_n-symmetric statistical systems*, Sov. Phys. JETP, **62**, 215-225, (1985).

A Dressed charge formalism

Following [6, 52, 24, 15] the finite size energy gaps of $\mathcal{H}_{\theta=0}$ for periodic boundary conditions are

$$\begin{aligned}\Delta E(\Delta N_\pm, Q_\pm) = \frac{2\pi}{\mathcal{L}} v_F \Big(&\frac{1}{4}(\Delta N_+, \Delta N_-)(\Xi^\top \Xi)^{-1}(\Delta N_+, \Delta N_-) \\ &+ (Q_+, Q_-)(\Xi^\top \Xi)(Q_+, Q_-) + \mathcal{N} \Big) + o(\mathcal{L}^{-1})\,.\end{aligned} \tag{25}$$

($\mathcal{N}$ being a non-negative integer). Taking into account that only $\pm$-strings are present in the ground state the 2×2 dressed charge matrix $\Xi = \xi(x)|_{x=\infty}$ is obtained from the linear integral equation

$$\begin{aligned}\xi(x) &= \begin{pmatrix} 1 & 0 \\ 0 & 1 \end{pmatrix} - \frac{1}{2\pi} \int_{-\infty}^{\infty} \mathrm{d}y\, \xi(y) K(y-x)\,, \\ K(x) &= \begin{pmatrix} k(x, \frac{1}{3}) & k(x, \frac{5}{6}) \\ k(x, \frac{5}{6}) & k(x, \frac{1}{3}) \end{pmatrix}, \quad k(x,t) = \frac{\sin(2\pi t)}{\cosh(x) - cos(2\pi t)}.\end{aligned} \tag{26}$$

Using Wiener Hopf techniques the dressed charge matrix can be expressed in terms of the Fourier transform of the kernel matrix giving

$$\Xi^\top \Xi = \Big(1 - \widetilde{K}(\omega = 0)\Big)^{-1} = \begin{pmatrix} 1 & \frac{1}{2} \\ \frac{1}{2} & 1 \end{pmatrix}. \tag{27}$$

Hence the scaling dimensions and conformal spins of primary operators in the effective field theory for $\mathcal{H}_{\theta=0}$ in terms of the quantum numbers $\Delta N_\pm$ and $Q_\pm$ characterising the corresponding excitation (22) are

$$\begin{aligned} X &= \frac{1}{3}\left((\Delta N_+)^2 - \Delta N_+\Delta N_- + (\Delta N_-)^2\right) + \left((Q_+)^2 + Q_+Q_- + (Q_-)^2\right) , \\ s &= -\frac{1}{2}\left(Q_+\Delta N_+ + Q_-\Delta N_-\right) . \end{aligned} \tag{28}$$

The $\Delta N_\pm \equiv N_\pm - \frac{\mathcal{L}}{2} \pm \frac{\mathcal{L}}{4}$ correspond to the change in number of $\pm$-strings (subject to the condition that the total number of roots is $\mathcal{L}$) as compared to the thermodynamic ground state while the $Q_\pm$ determine the momentum of the excitation. For a configuration with $n_\pm$ Bethe roots at $\pm\infty$ they can take discrete values

$$Q_\pm \equiv \frac{1}{3}(n_{+\infty} - n_{-\infty}) \pmod 1.$$

For a given solution $\{x_k^\pm\}$ of the Bethe equations the $Q_\pm$ can also be determined numerically using the counting functions defined above:

$$Q_\pm = \frac{1}{N_\pm}\sum_{k=1}^{N_\pm} Z_\pm(x_k^\pm) .$$

Due to the discrete set of possible values for $Q_\pm$ the data for systems with $\mathcal{L} \leq 10$ are sufficient to identify the quantum numbers for the lowest finite size gaps of $\mathcal{H}_{\theta=0}$, see in Table 11. The observed dimensions support our identification of the critical theory with a Z_4 parafermion.

Table 11: The lowest excitations of $\mathcal{H}_0$ in terms of the quantities $\Delta N_\pm$ and $Q_\pm$ for different chain lengths.

$\mathcal{L}$ mod 4	X	s	ΔN_+	ΔN_-	ΔQ_+	ΔQ_-
0	0	0	0	0	0	0
	$\frac{1}{3}$	$-\frac{1}{3}$	0	-1	$-\frac{1}{3}$	$+\frac{2}{3}$
	$\frac{2}{3}$	0	0	-2	0	0
	$\frac{1}{6}$	0	-1	-1	0	0
1	$\frac{1}{16}$	$\frac{1}{16}$	$-\frac{1}{4}$	$+\frac{1}{4}$	$+\frac{1}{4}$	$-\frac{1}{4}$
	$\frac{7}{48}$	$-\frac{1}{48}$	$-\frac{1}{4}$	$-\frac{3}{4}$	$-\frac{5}{12}$	$+\frac{1}{12}$
	$\frac{19}{48}$	$-\frac{13}{48}$	$-\frac{1}{4}$	$-\frac{3}{4}$	$+\frac{7}{12}$	$-\frac{11}{12}$
2	$\frac{1}{12}$	$-\frac{1}{12}$	$-\frac{1}{2}$	$-\frac{1}{2}$	$-\frac{1}{6}$	$-\frac{1}{6}$
	$\frac{5}{12}$	$-\frac{1}{4}$	$-\frac{1}{2}$	$-\frac{3}{2}$	$-\frac{1}{2}$	$+\frac{1}{2}$